

BIROn - Birkbeck Institutional Research Online

Li, S. and Najman, Y. and Vermeesch, P. and Barfod, D.N. and Millar, I. and Carter, Andrew (2024) A critical appraisal of the sensitivity of detrital Zircon U–Pb provenance data to constrain drainage network evolution in Southeast Tibet. *Journal of Geophysical Research: Earth Surface* 129 (2), ISSN 0148-0227.

Downloaded from: <https://eprints.bbk.ac.uk/id/eprint/53260/>

Usage Guidelines:

Please refer to usage guidelines at <https://eprints.bbk.ac.uk/policies.html>
contact lib-eprints@bbk.ac.uk.

or alternatively



RESEARCH ARTICLE

10.1029/2023JF007347

Special Section:

Controls and Biasing Factors in Sediment Generation, Routing, and Provenance: Models, Methods, and Case Studies

Key Points:

- Detrital zircon U–Pb source signatures for various terranes of southeastern Tibet are indistinguishable
- Sedimentary recycling limits the utility of detrital zircon U–Pb approach to determine the palaeodrainage evolution of southeastern Tibet
- Sr–Nd isotopes and mica $^{40}\text{Ar}/^{39}\text{Ar}$ ages may be potential alternative provenance tools for paleodrainage reconstruction

Supporting Information:

Supporting Information may be found in the online version of this article.

Correspondence to:

S. Li and Y. Najman,
lsh917@mail.iggcas.ac.cn;
y.najman@lancaster.ac.uk

Citation:

Li, S., Najman, Y., Vermeesch, P., Barfod, D. N., Millar, I., & Carter, A. (2024). A critical appraisal of the sensitivity of detrital zircon U–Pb provenance data to constrain drainage network evolution in southeast Tibet. *Journal of Geophysical Research: Earth Surface*, 129, e2023JF007347. <https://doi.org/10.1029/2023JF007347>

Received 19 JUL 2023

Accepted 8 JAN 2024

Author Contributions:






Conceptualization: Shihu Li, Yani Najman

Data curation: Shihu Li, Pieter Vermeesch, Dan N. Barfod, Ian Millar, Andy Carter

© 2024. The Authors.

This is an open access article under the terms of the [Creative Commons Attribution License](https://creativecommons.org/licenses/by/4.0/), which permits use, distribution and reproduction in any medium, provided the original work is properly cited.

A Critical Appraisal of the Sensitivity of Detrital Zircon U–Pb Provenance Data to Constrain Drainage Network Evolution in Southeast Tibet

Shihu Li^{1,2} , Yani Najman² , Pieter Vermeesch³ , Dan N. Barfod⁴, Ian Millar⁵ , and Andy Carter³ 

¹State Key Laboratory of Lithospheric Evolution, Institute of Geology and Geophysics, Chinese Academy of Sciences, Beijing, China, ²Lancaster Environment Centre, Lancaster University, Lancaster, UK, ³Department of Earth Sciences, University College London, London, UK, ⁴NEIF Argon Isotopes, University of Glasgow, SUERC, Glasgow, UK, ⁵Geochronology and Tracers Facility, British Geological Survey, Nottingham, UK

Abstract Provenance tools, particularly detrital zircon U–Pb analysis, have been widely employed to test drainage network evolution in southeast Tibet and its linkage with the growth of the Tibetan Plateau. Numerous provenance studies have been conducted on the sediments in the paleo-Yangtze and paleo-Red River drainage basins. Nevertheless, it is still hotly debated as to whether a “Mississippi” (dendritic) pattern Greater paleo-Red River, originating from southeast Tibet and draining to the South China Sea, existed in the early Cenozoic, and was subsequently captured by the paleo-lower Yangtze due to uplift of southeastern Tibet. In this study, in addition to presenting new data from the Gonjo and Jianchuan basins along which the Greater paleo-Red River is proposed to have flowed, we compiled all the published detrital zircon U–Pb data from the paleo-upper Yangtze and paleo-Red River drainage basins from Triassic and younger rocks. Our large database of detrital zircon U–Pb analyses shows that the different terranes in the paleo-upper Yangtze and paleo-Red River drainage basins have similar zircon U–Pb signatures since the Late Triassic closure of the Paleo-Tethys Ocean. Therefore, most of the sediments in the Cenozoic sedimentary basins in southeast Tibet could have been either deposited by long-distance transport in large rivers from southeast Tibet or recycled from local bedrock. Given the potential importance of sedimentary recycling that we have demonstrated, this poses challenges to the use of detrital zircon U–Pb analyses to determine paleodrainage in this region. We therefore further explored the previously relatively limited use of Sr–Nd isotopes on mudstones and detrital mica $^{40}\text{Ar}/^{39}\text{Ar}$ ages, with new analyses from the Gonjo and Jianchuan Basins, to determine if these techniques were better suited to reconstruct paleodrainage evolution. Whilst these techniques do show some promise, more analyses and strategic sampling are required to obtain a full understanding of the extent of their potential utility. Overall, our integrated provenance study indicates that the available data are not sufficiently conclusive to support or refute the Greater paleo-Red River capture model.

Plain Language Summary In the southeast margin of the Tibetan Plateau, five large-scale rivers (Yangtze, Mekong, Salween, Irrawaddy, and Yarlung-Brahmaputra) flow through central Tibet to southeast Asia. How these rivers evolved during the Cenozoic uplift of the Tibetan Plateau remains a controversial issue. It has been hypothesized that, in the early Cenozoic, all the upper reaches of the five rivers flowed to the south and connected to the Red River flowing to the South China Sea, forming a “Mississippi” pattern Greater paleo-Red River; this Greater paleo-Red River was later captured by the lower Yangtze due to uplift of the Tibetan Plateau. Here we test the Greater paleo-Red River model by adding new data from Cenozoic sedimentary basins and providing a comprehensive compilation of available detrital zircon U–Pb data from different terranes of southeast Tibet. With this large data set, we found that the source signatures for the various terranes from southeast Tibet are indistinguishable due to zircon recycling. Moreover, we explored the use of Sr–Nd isotopes and detrital mica $^{40}\text{Ar}/^{39}\text{Ar}$ ages as potential alternative provenance tools to test the river capture model. The overall provenance data are insufficient to test the validity of the Greater paleo-Red River capture model.

1. Introduction

Tectonic uplift, climate change, river erosion, and alluvial deposition are fundamental processes that have shaped the present landscape. Fluvial systems respond rapidly to climate change and/or tectonic events, as reflected in

Funding acquisition: Shihu Li, Yani Najman
Investigation: Shihu Li, Yani Najman, Pieter Vermeesch
Methodology: Shihu Li
Project Administration: Shihu Li, Yani Najman
Resources: Shihu Li
Supervision: Yani Najman
Writing – original draft: Shihu Li, Yani Najman
Writing – review & editing: Shihu Li, Yani Najman, Pieter Vermeesch, Dan N. Barfod, Ian Millar, Andy Carter

lateral channel shifting, headward erosion, ridge migration, and river captures, which are major influences on the development of the topography we see today. Therefore, deciphering paleodrainage network evolution is a fundamental approach to constraining the influence of tectonic evolution and climate change on an area.

A type example for understanding the dynamic response of drainage network evolution to mountain uplift or climate change lies in southeast Tibet where five major rivers (the Yarlung-Brahmaputra, Irrawaddy, Salween, Mekong, and Yangtze) flow (e.g., Clark et al., 2004; Clift, Blusztajn, & Duc, 2006; Clift, Carter, et al., 2006; Nie et al., 2018; Figure 1). These rivers have very unusual geometries. The Yarlung–Tsangpo River originates in the western Lhasa terrane and flows eastward along the Yarlung–Tsangpo suture along which India collided with Asia. The river turns sharply to the south at the Eastern Himalayan Syntaxis and changes direction again to flow southwestward after its confluence with the Brahmaputra River. All three rivers of the Salween, Mekong, and Yangtze originate from the eastern part of central Tibet and flow eastward. After approaching the Eastern Himalayan Syntaxis, they flow in parallel to the south for at least 200 km (known as “The Three Parallel Rivers,” Figure 1b), with their drainage basins in much closer proximity than would be expected from rivers of their size. The most striking geometry is that of the Yangtze River, which exhibits a sharp turn at Shigu, that is, the First Bend of the Yangtze (Figure 1), where the flow direction changes from southeastward to northeastward. These unusual geometries, together with the long wide valley just south of the First Bend of the Yangtze (considered as an abandoned river course (e.g., Barbour, 1936; Lee, 1934)) and the southward flowing Red River (Figure 1b), make river capture of a paleo-upper Red River (including the upper Yangtze (also called the Jinsha River), and possibly the upper Salween and upper Mekong) by the paleo-lower Yangtze, a plausible and intuitive explanation to explain the current drainage pattern (e.g., Brookfield, 1998; Clark et al., 2004).

This drainage network and its development receives particular attention with respect to its link with understanding mechanisms of Tibetan evolution and the potential use of drainage changes to constrain the timing of plateau uplift (Cao et al., 2018; Clark et al., 2004; Hallet & Molnar, 2001; Yang et al., 2015; Yuan et al., 2021; Zhao et al., 2021). This is of particular value given the complexities and uncertainties in timing of southeastern plateau uplift as determined from low temperature thermochronology, regional tectonics, and paleoaltimetry studies, with proposed uplift time ranging from Late Cretaceous to Late Miocene (e.g., Cao et al., 2020; Clark et al., 2005; Hoke et al., 2014; Li, Su, et al., 2020; Liu-Zeng et al., 2018; McPhillips et al., 2016; Nie et al., 2018; Su et al., 2019; Tian et al., 2018, 2022; H. Zhang et al., 2016). Hallet and Molnar (2001) proposed that the large river drainages in the region are antecedent, and their unusual geometries are the result of tectonic deformation by horizontal shear and crustal shortening. By contrast, Clark et al. (2004) proposed that the present drainage configuration is the result of various river captures and drainage reversals away from previous continental-scale drainage formed at low elevation (Figure 2); they proposed that the timings of these river captures constrain the timing of eastern Tibetan uplift due to lower crustal flow. However, Yang et al. (2015) suggested that the regional river network was disrupted by tectonic deformation when the region was already at altitude. More recently, Fox et al. (2020) demonstrated that the assumption of a low-relief surface that has been uplifted and dissected is problematic and highlighted the need to improve understanding of spatial variations in erodibility including drivers linked to climate change and drainage capture events.

Provenance studies, such as those using the techniques of U–Pb dating of detrital zircon, $^{40}\text{Ar}/^{39}\text{Ar}$ dating of detrital mica, Sr–Nd bulk rock characterization, and K-feldspar Pb characterization, have been applied to rocks considered to be paleo-river sediments in southeast Tibet to detect possible provenance changes due to river capture and thereby test the river capture models (e.g., Chen et al., 2017; Clift, Blusztajn, & Duc, 2006; Clift, Carter, et al., 2006; Clift et al., 2004, 2008, 2020; Deng et al., 2018, 2020; Hoang et al., 2009; Kong et al., 2009, 2012; Wissink et al., 2016; Yan et al., 2012; Z. Zhang, Daly, Li, et al., 2021; Z. Zhang et al., 2014; H. Zhang et al., 2016; Z. Zhang et al., 2017; Y. Zhang et al., 2018; P. Zhang et al., 2019 and references therein; Cao et al., 2023; Fan et al., 2005; Feng et al., 2021; Fu et al., 2021; He et al., 2021; Jiao et al., 2022; Sun et al., 2020a, 2020b, 2020c, 2021; Yang et al., 2020; Y. Zhang et al., 2019; Z. Zhang et al., 2022, 2023; Zhao et al., 2021).

Although numerous provenance data have been reported, especially from the most widely employed detrital zircon U–Pb approach, no consensus has been reached. Interpretations can be summarized into two schools of thought. The first school of thought, based on the similar detrital zircon U–Pb spectra between the potential sources of southeastern Tibet and the Cenozoic basins in southeast Tibet, argues that the provenance studies support a connection between the paleo-upper and -middle Yangtze, the paleo-upper Mekong, -upper Salween, and the paleo-Red River, that is, the Greater paleo-Red River, which was captured later by the paleo-lower

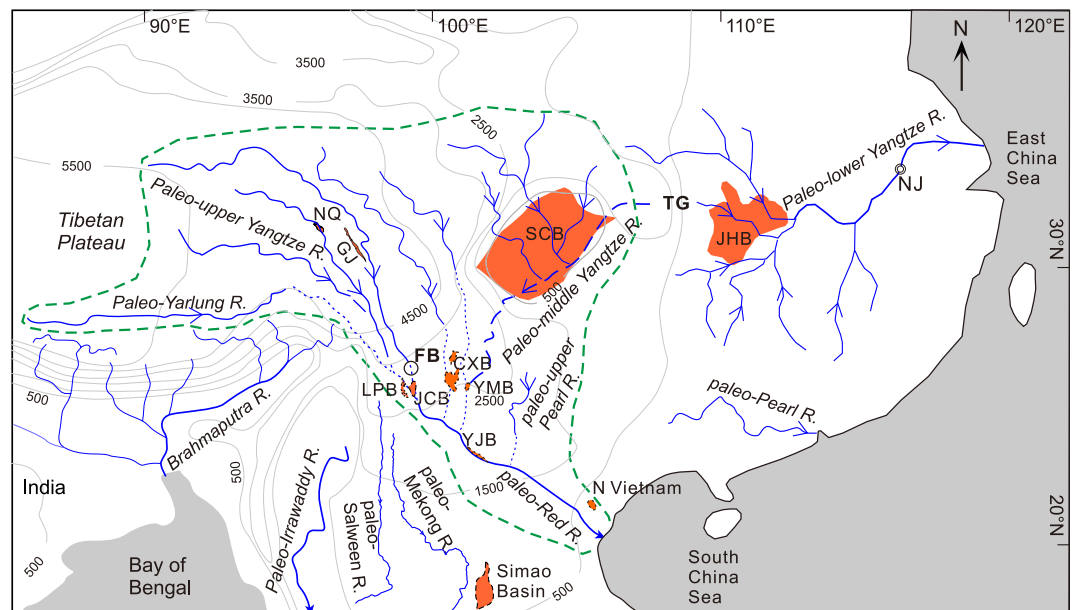


Figure 2. The Greater paleo-Red River (green dashed area) capture model proposed by Clark et al. (2004). The orange areas denote the main sedimentary basins discussed in this study. Modified after Clark et al. (2004) and P. Zhang et al. (2019), Y. Zhang et al. (2019). NQ: Nangqian Basin, GJ: Gonjo Basin, FB: the First Bend of Yangtze, LPB: Lanping Basin, JCB: Jianchuan Basin, CXB: Chuxiong Basin, YMB: Yuanmou Basin, YJB: Yuanjiang Basin, N Vietnam: North Vietnam Basin, SCB: Sichuan Basin, TG: Three Gorges, JHB: Jiangnan Basin, NJ: Nanjing.

et al., 2021; Gourbet et al., 2017; He et al., 2021; Yan et al., 2012; Zheng et al., 2021). We collected data from the Gonjo Basin because it is located in eastern Tibet (Figure 2), and the massive red beds in the basin are debatably regarded as the fluvial remnants of the paleo-upper Yangtze (Zheng, 2015), which suggests that the paleo-upper Yangtze was already developed during the deposition of the Gonjo Basin.

Furthermore, given the challenges of using detrital zircon U–Pb data to determine the evolution of the Yangtze and Red rivers, as shown in this study, we also carried out a pilot study applying Sr–Nd whole rock and detrital mica $^{40}\text{Ar}/^{39}\text{Ar}$ analyses to rocks of the Gonjo and Jianchuan Basins to test whether they might provide good approaches for source discrimination, and hence paleo-drainage reconstruction. Finally, based on all the compiled provenance data sets, we comment on the implications for paleodrainage network evolution in southeast Tibet and future detrital zircon U–Pb studies.

2. Are the Different Terranes of Southeastern Tibet Distinguishable in Terms of Zircon U–Pb Spectra?

East and southeast Tibet consist of a series of mosaic blocks that were amalgamated during the opening and closure of the intervening Tethyan oceans. These blocks include the Songpan–Ganzi, Yidun Arc, east and west Qiangtang, Indochina, Sibumasu, and Lhasa terranes (Figure 1a). Based on paleomagnetic and geological constraints, east Qiangtang–Indochina collided with North and South China blocks by closing the north branch of the Paleo-Tethys Ocean during the Middle-Late Triassic (e.g., Ding et al., 2013; Guan et al., 2021; Huang et al., 2018; Pullen et al., 2008; Song et al., 2015; Wu et al., 2020; Yan et al., 2019), forming the Songpan–Ganzi flysch as a remnant oceanic basin (Nie et al., 1994; Zhou & Graham, 1996). In the Late Triassic, west Qiangtang–Sibumasu collided with east Qiangtang–Indochina due to the closure of the southern branch of the Paleo-Tethys Ocean (e.g., Zhao et al., 2015). These events are referred to as the Indosinian Orogeny (e.g., Carter et al., 2001). The Lhasa terrane collided with Qiangtang during the Late Jurassic–Early Cretaceous (Li et al., 2019; Ma et al., 2018). These above-mentioned collisions, together with the final collision between India and Asia in the early Cenozoic, created the Tibetan Plateau region.

To robustly test the drainage capture and evolution model by using detrital zircon U–Pb geochronology, the potential source signatures from the different terranes of southeastern Tibet through which the Yangtze and

Red rivers flow must be clearly distinguishable. Since the modern upper Yangtze drains the east Qiangtang and Songpan-Ganzi terranes, whilst the Red River headwaters drain the Indochina terrane and South China Block, it has been argued that if one observes zircon signatures from the Songpan-Ganzi, or east Qiangtang terranes in the Cenozoic rocks of Greater paleo-Red River drainage basins, then a through-flowing river existed from eastern Tibet, connecting the Red River to the South China Sea.

In previous studies, the characteristic source signatures from these terranes were generally composed of a compilation of zircon U–Pb ages from igneous rocks (e.g., Clift et al., 2008; He et al., 2014). However, we consider that this may ignore the contribution of zircons from sedimentary rocks in these terranes, to the overall terrane signature. Such a contribution is potentially significant as most of the area in these terranes is covered by sedimentary rocks. Therefore, a more representative signature for a terrane may be gained by compiling information from older sedimentary rocks in that terrane. Given that the different terranes in southeast Tibet were amalgamated after the Middle-Late Triassic (e.g., Ding et al., 2013; Faure et al., 2018; Guan et al., 2021; Pullen et al., 2008; Song et al., 2015), we compiled all available detrital U–Pb zircon grains ($n = 29,545$) from sedimentary basin rocks dated from the Middle-Late Triassic in the east Qiangtang terrane, Yidun Arc terrane, Songpan-Ganzi terrane, Indochina terrane, and South China Block (Sichuan Basin and Chuandian sub-terrane) (see Figure S1 in Supporting Information S1 for data locations and Table S1 in Supporting Information S2 for details). These are all the basins available to characterize the terranes over which the paleo-upper Yangtze and paleo-Red River flowed. Since we compile the sedimentary bedrock around the Cenozoic basins, this approach can detect if the Cenozoic basin rocks in the Greater paleo-Red River drainage basins may have been locally sourced, as Wissink et al. (2016) suggested.

From the visual comparison of Kernel density estimation (KDE, Figure 3) using an adaptive bandwidth (same as the other KDE figures) and (nonmetric) multidimensional scaling (MDS, Vermeesch, 2013) plots with bootstrapped confidence regions of the terranes (Figure S2 in Supporting Information S1), we note that in most cases, from Late Triassic time onwards, sedimentary rocks from different terranes in southeast Tibet show similar zircon age populations. The five dominant age groups of 200–300, 400–500, 700–1,100, 1,700–1,900, and 2,400–2,600 Ma are common peaks in East Asia, associated with the Indosinian, Caledonian, Jinning, Lvliang, and Wutai orogenies, respectively (Wu et al., 2019).

Late Triassic and younger sedimentary rocks cover a significant spatial extent of the various terranes in southeast Tibet, and therefore contribute significant detritus to the Cenozoic sediments. Thus our compilation, which shows that rocks younger than the Late Triassic from the different terranes in southeast Tibet have similar zircon age populations by sedimentary recycling, makes it difficult to obtain a characteristic source signature for these terranes. We illustrate the implications of this proposal in more detail below by adding new data and a comprehensive review from critical regions of the Gonjo and Jianchuan basins along the length of the drainage route.

The similarity of zircon U–Pb signatures in Late Triassic and younger sedimentary rocks has implications for previous provenance studies. Many previous studies have found that the Cenozoic sedimentary rocks from a series of basins, for example, Simao, Jianchuan, and Northern Vietnam basins have zircon ages similar to the Late Triassic rocks in Songpan-Ganzi or eastern Qiangtang terranes. This has been used as evidence to support the existence of a paleo-upper Yangtze that originated from eastern Tibet and connected to the paleo-Red River in the Early Cenozoic (e.g., Chen et al., 2017; Clift et al., 2020; Kong et al., 2012; Yan et al., 2012; Zheng et al., 2021). However, we suggest that the zircon signature in these basins could also be locally derived by recycling of surrounding older (e.g., Late Triassic–Cretaceous) sedimentary sequences, a proposition recently proposed by Z. Zhang et al. (2023).

We note that Clift et al. (2020) observed that many sedimentary rocks in Cenozoic basins of southeastern Tibet and sediments in rivers of SE Asia contain significant Cenozoic detrital zircon U–Pb aged grains. They argued that these Cenozoic zircon grains can only be sourced from the Qamdo Block (the east Qiangtang terrane in this study) in east Tibet, without recycling, and therefore can be used as a characteristic source signature for a through-flowing river from eastern Tibet. Guo et al. (2021) also used the appearance of Cenozoic detrital zircon U–Pb ages in Miocene sediments of the Jiangnan Basin (see Figure 2 for location) as evidence for the formation of the modern Yangtze. However, as shown in the Jianchuan Basin (see Section 4), Cenozoic volcanic rocks are also widespread in Yunnan Province (Chung et al., 2005), and even in the South China Block (e.g., Nanjing area, Figure 2 for location (Zheng et al., 2013)), suggesting that the Cenozoic zircon grains are also not diagnostic signatures of eastern Tibet.

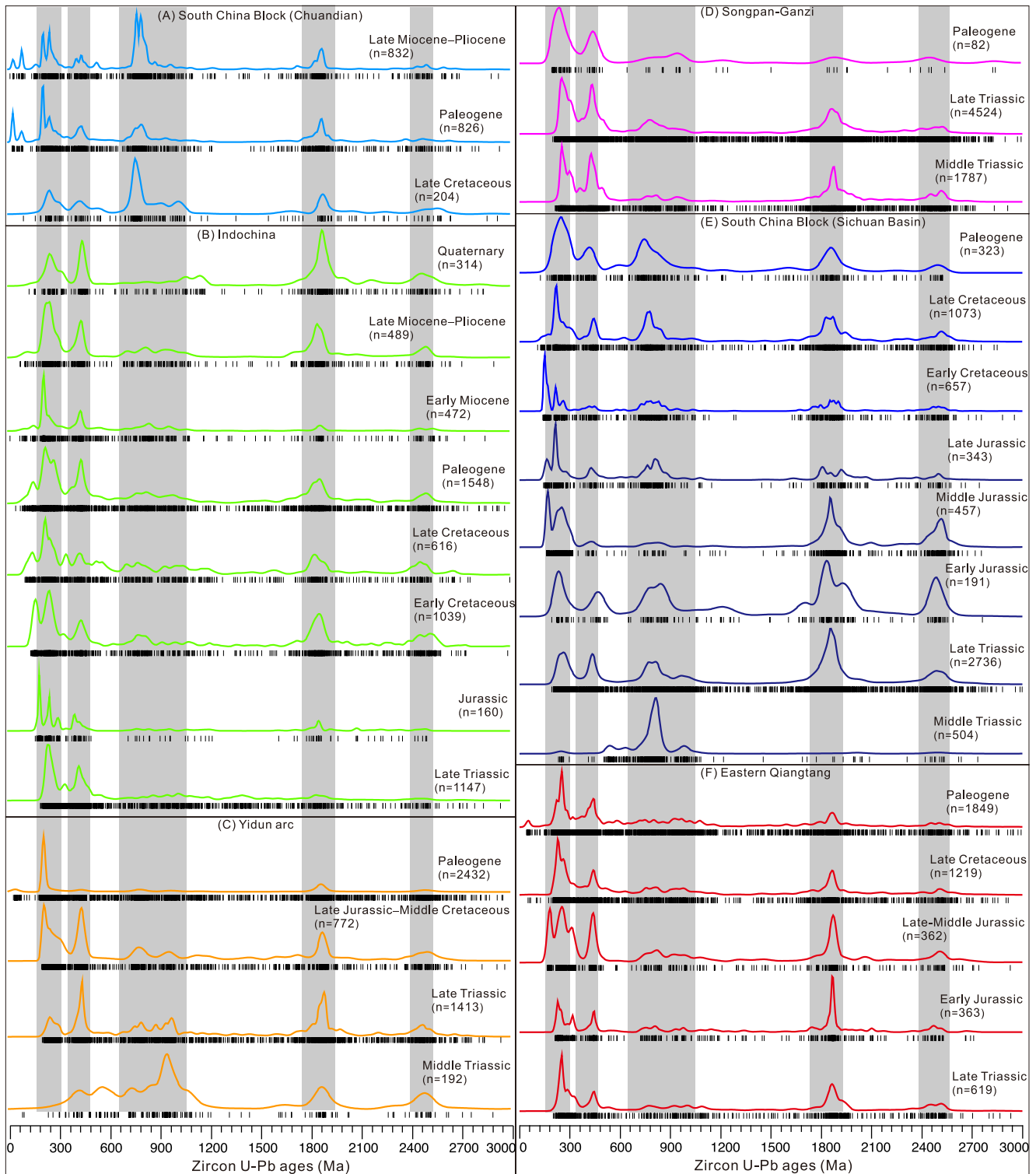


Figure 3. Kernel Density Estimation (KDE) plots for the compiled U-Pb detrital zircon data from different geological domains on the eastern margin of Tibet. The five gray bars indicate the common zircon populations seen in East Asia, associated with the Indosinian orogeny, Caledonian orogeny, Jinning orogeny, Lvliang orogeny, and Wutai orogeny, respectively (Wu et al., 2019). Data used in the compilation are referenced in Supporting Information S2.

The sedimentary rocks in the Yidun Arc and South China Sichuan Basin (Figures 3c and 3e) show a significant change in the detrital zircon U–Pb signature between the Middle and Late Triassic, shifting from more restricted to more diverse spectra, although this change is not seen in the Songpan-Ganzi terrane. This change may relate to the continued amalgamation of terranes within the Paleo-Tethys Ocean during the Triassic, as discussed above (e.g., Ding et al., 2013; Faure et al., 2018; Pullen et al., 2008; Yan et al., 2019), which may have had a significant influence on sediment routing. Rivers dynamically respond to associated tectonic shortening, concentrating erosion on newly uplifted areas and building new pathways that span the newly accreted terranes, broadening the potential for changes and diversification of provenance. This is evidenced, for example, in the southwestern Sichuan Basin where Yan et al. (2019) noted a major change in sediment routing in response to the Late Triassic closure of the Paleo-Tethys Ocean that drove shortening across the Longmen Shan thrust belt and the eastern Songpan-Ganzi terrane. The zircon U–Pb ages in the Lower–Middle Triassic samples are dominated by Neoproterozoic (~700–900 Ma) zircons sourced mainly from the southwestern South China basement. By contrast, the Upper Triassic samples record multiple peaks, diagnostic of sources within the Qinling, Longmen Shan and Songpan-Ganze terranes (e.g., age peaks at ~270, ~435, ~775, ~1,010, ~1,840 and ~2,480 Ma). However, we acknowledge that the difference may also result from the significant difference in the number of grains/samples analyzed between Early-Mid and Late Triassic samples. More pre-Late Triassic analyses from a number of different terranes would be needed to test this hypothesis further.

3. Does the Gonjo Basin Sedimentary Succession Represent Deposits of the Paleo-Upper Yangtze as Indicated by Detrital Zircon U-Pb?

3.1. Age, Sedimentology and Previous Interpretations Regarding the Gonjo Basin Sedimentary Rocks

The >200 km long Gonjo Basin (30.85°N, 98.3°E, Figure 4) is located in the eastern part of central Tibet, at the boundary between the Qiangtang and Songpan-Ganzi terranes. It is one of many thrust-bounded basins (e.g., Hoh Xil and Nangqian basins) in the region and is interpreted to have formed as a syn-contractual basin in the footwall of the Yangla fold-thrust system (Li, van Hinsbergen, Najman, et al., 2020; Li, Hinsbergen, Shen, et al., 2020; Studnicki-Gizbert et al., 2008; Tang et al., 2017). The sedimentary strata of the basin are now exposed in an asymmetric syncline, and mainly consist of red-colored mudstones, sandstones, and rare conglomerates, reaching a total thickness of >3,000 m (Li, van Hinsbergen, Najman, et al., 2020; Studnicki-Gizbert et al., 2008; Tang et al., 2017), and were interpreted as a mixed depositional environment of alluvial fan, fan-delta, floodplain, and lacustrine facies (Studnicki-Gizbert et al., 2008). The sedimentary sequence is divided into the Gonjo Formation and Ranmugou Formation, where the latter is further sub-divided into lower, middle, and upper parts.

The Gonjo Basin was previously assigned an Eocene age based on flora and pollen fossils observed at the top of the succession (Bureau of Geology and Mineral Resources of Xizang (Tibet) Autonomous Region, 1993). However, recent U–Pb and $^{40}\text{Ar}/^{39}\text{Ar}$ dating on interbedded volcanic rocks (Studnicki-Gizbert et al., 2008; Tang et al., 2017), U–Pb detrital zircon data from sandstones (Xiong et al., 2020; Y. Zhang et al., 2018), together with high-resolution magnetostratigraphy, precisely constrain the Gonjo Basin deposition from 69 to 41.4 Ma (Li, van Hinsbergen, Najman, et al., 2020), although Xiao et al. (2021) suggested that the Gonjo Basin ceased deposition in its central part at ~50 Ma.

The current upper Yangtze River roughly flows N-S ~50 km east of the Gonjo Basin, along the Jinsha suture separating the Qiangtang and Yidun Arc terranes. Three Yangtze tributaries flowing south, east, and north to the Gonjo Basin converge in the central part of the basin and then flow to the east to join the Yangtze River (Figure 4b). Based on detailed sedimentologic, stratigraphic, and structural studies of the Gonjo and nearby Nangqian basins, Horton et al. (2002) and Studnicki-Gizbert et al. (2008) concluded that both basins were fed by proximal sources and therefore the large through-going rivers of the Yangtze and Mekong were not developed until the deposition ceased in these basins in the Late Eocene. However, Zheng (2015) proposed that the massive red beds in the Gonjo Basin of eastern Tibet are the fluvial remnants of the paleo-upper Yangtze, which suggests that the paleo-upper Yangtze was already developed since the Eocene. He suggested that this paleo-upper Yangtze could have connected to the paleo-Red River. These ideas are consistent with later detrital zircon studies (He et al., 2021; Zheng et al., 2021) which showed that the zircon U–Pb spectra from the Paleocene-Eocene rocks of the Gonjo and Jianchuan basins (Figure 2), which are proposed to both be paleo-upper Yangtze deposits (Zheng, 2015), look similar to each other and to the Songpan-Ganzi terrane. Y. Zhang et al. (2019) albeit also suggested that the Gonjo Basin sediments were mainly sourced from the nearby Songpan-Ganzi terrane, but

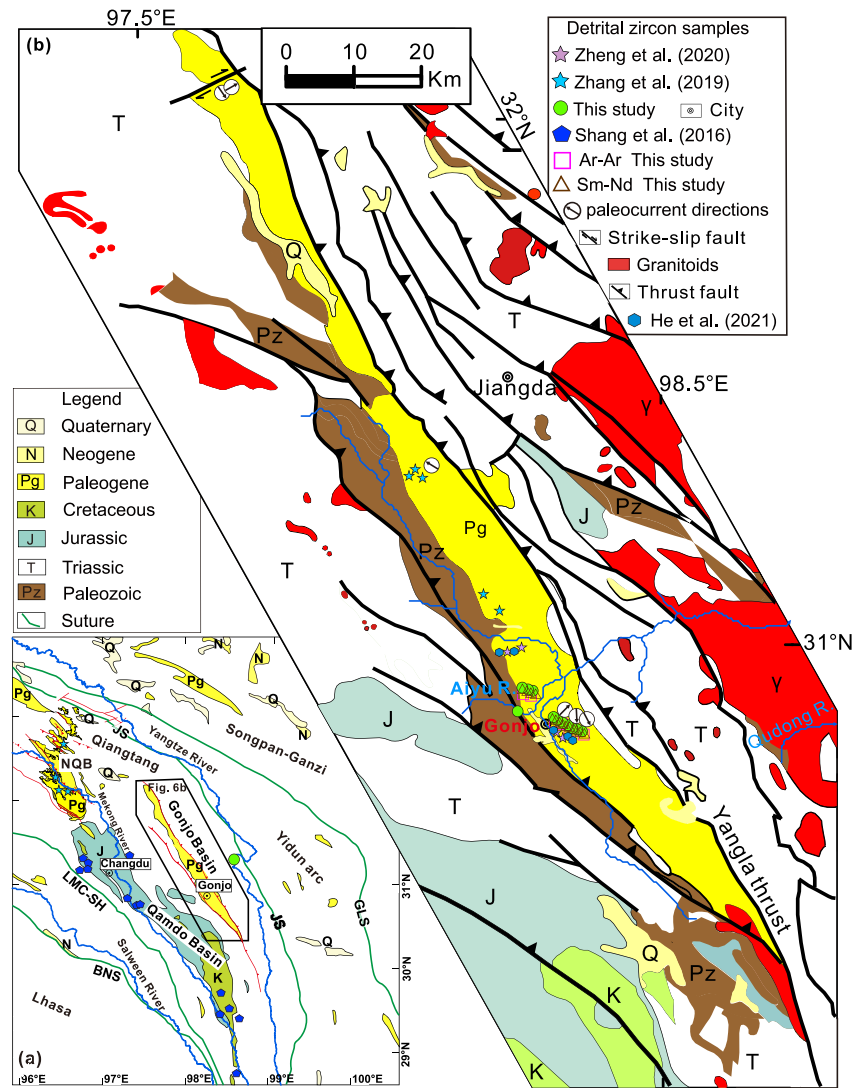


Figure 4. (a) Geological map of southeastern Tibet showing the Gonjo and Nangqian basins. (b) Enlarged geological map of the Gonjo Basin showing the locations of U–Pb sampling sites of previous work and this study. Arrows with circles denote the paleocurrent directions; data are from Studnicki-Gizbert et al. (2008) and Tang et al. (2017). The abbreviations are the same as Figures 1 and 2.

argued that the Gonjo Basin was an internally drained basin. In this scenario, the upper Yangtze was not established during the Late Cretaceous–Eocene deposition of Gonjo Basin sediments.

3.2. Provenance of the Gonjo Basin Based on Detrital Zircon U–Pb Data

In order to explore the drainage scenarios based on provenance data derived from detrital zircon U–Pb spectra, as summarized above, we carried out detrital zircon U–Pb analyses from 12 sandstone samples along the magnetostratigraphic section of Li, van Hinsbergen, Najman, et al. (2020), with all samples separated by an interval of 2–4 Ma (Figure 4b). We also analyzed two modern river sediments, one from the modern Yangtze near Gonjo, and one from the eastern side of the Gonjo Basin that drains into the Gonjo Basin (sample Aiyu River, see Figure 4b for location). Sampling details, U–Pb methods and results are provided in Table S1–S3 of the Supporting Information S2, respectively. Moreover, we compiled all the published detrital zircon data from the Gonjo Basin.

As shown in Figure 5, except for one sample SY-9 from the upper Ranmugou Formation, all other samples show similar zircon U–Pb age spectra with minor variations. Most samples show five age groups of 200–300, 400–500,

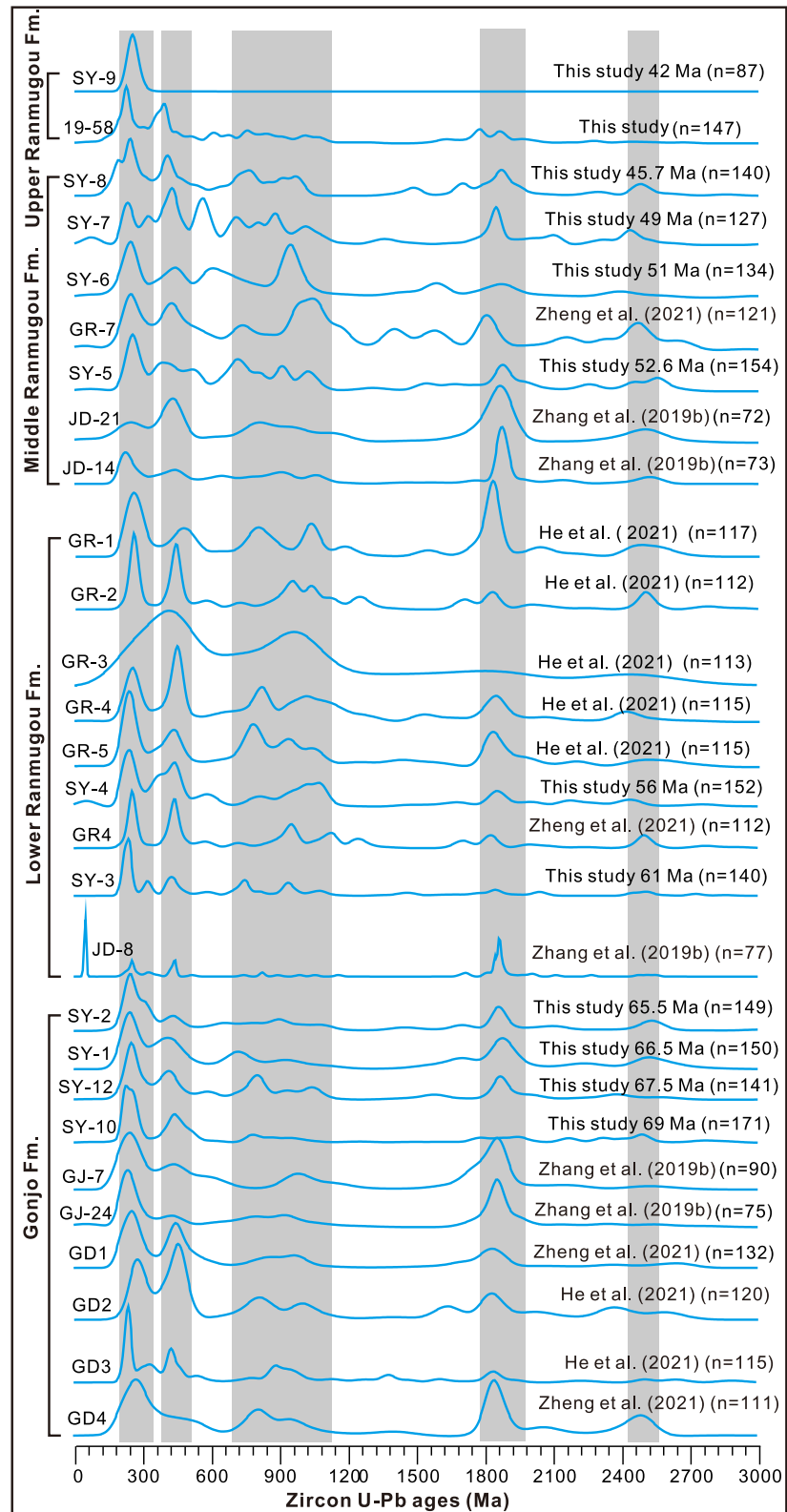


Figure 5. KDE plots of all detrital zircon U-Pb ages from sedimentary rocks of the Gonjo Basin in stratigraphic order, including published data as referenced. The gray vertical bars indicate the common zircon populations in East Asia, as stated in Figure 3.

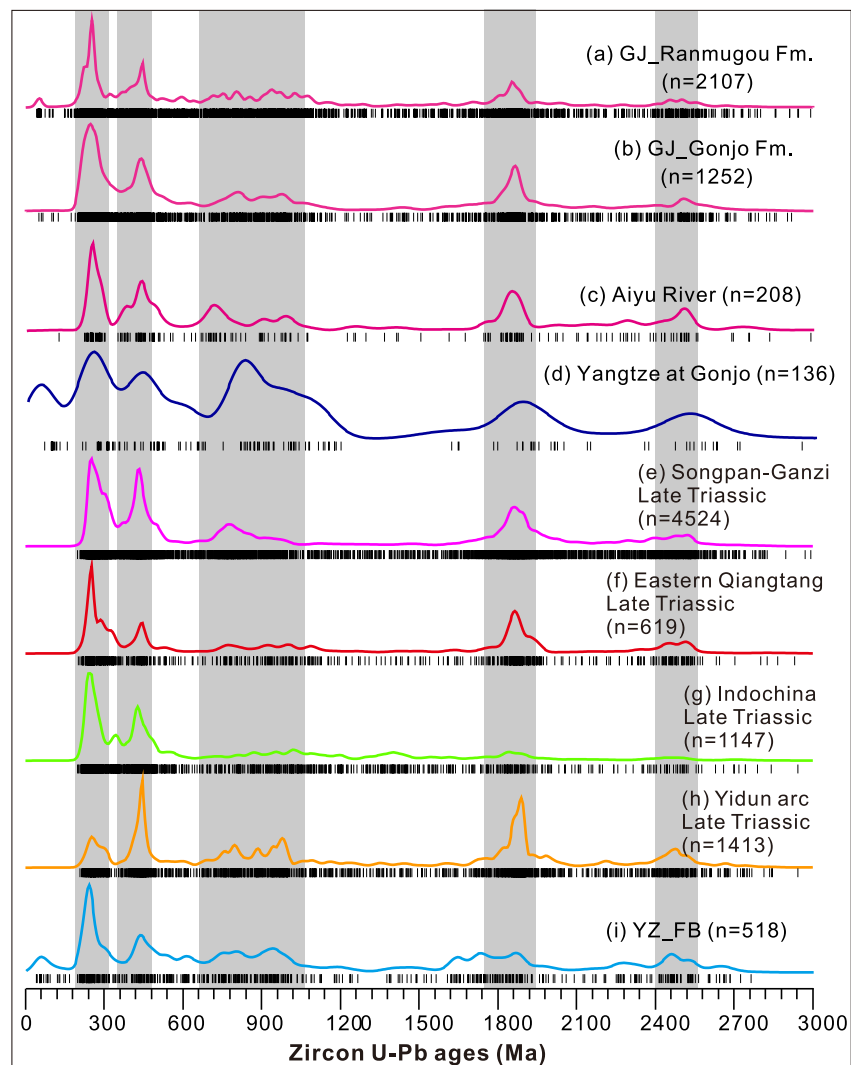


Figure 6. Detrital zircon U–Pb data from the Gonjo Basin compared to various source regions. KDE plots of detrital zircon U–Pb ages from the Gonjo Basin (GJ) Gonjo (a) and Ranmugou (b) formations, compared to modern local rivers draining into the Gonjo Basin from the underlying Qiangtang terrane (Aiyu River, c), modern river sediment from the Yangtze River at Gonjo (d), Late Triassic sedimentary rocks from East Asian terranes (e–h), and modern river First Bend of Yangtze (YZ_FB, i).

700–1,100, 1,700–1,900, and 2,400–2,600 Ma; some samples also have a Cenozoic age group of 50–60 Ma. Since there are no significant variations of detrital zircon U–Pb spectra over the deposition of the Gonjo Basin, we amalgamated the data into the Late Cretaceous Gonjo Formation, and the Early Cenozoic Ranmugou Formation, and compared them with the potential source signatures.

From a visual comparison of the KDE (Figure 6) and MDS (Figure S3 in Supporting Information S1) plots, we show that, apart from a minor 60 Ma age population, the detrital zircon U–Pb age spectra from the compiled Gonjo and Ranmugou formations are similar to the Late Triassic Songpan-Ganzi terrane. The Gonjo and Ranmugou formations are also similar to the First Bend of the modern Yangtze. This could suggest that a paleo-upper Yangtze River, which originated from the Songpan-Ganzi terrane and flowed through the Gonjo Basin to the First Bend, existed in the Eocene, as proposed by Zheng et al. (2021). However, the zircon age spectrum in particular of the Gonjo Formation is also similar to that of the eastern Qiangtang Cretaceous bedrock and to that of the local modern Aiyu River, a small tributary that only cuts through the Triassic and Paleozoic bedrocks to the east of Gonjo Basin (Figure 4b), demonstrating that a local provenance, for example, the Qamdo Basin in the southwest (Figure 4a), could also well explain these Gonjo Basin data. For the 50–60 Ma age population present in the

Gonjo Basin, we propose that it could be derived from the surrounding area since magmatic rocks of this age are widespread in the east Qiangtang terrane (e.g., Chung et al., 2005).

In summary, the large compiled detrital zircon data set from the Gonjo Basin could represent the derivation of grains from the Songpan-Ganzi terrane, which could support the concept of a major Eocene River in the region, consistent with the idea that a paleo-upper Yangtze River originated from eastern Tibet at that time (e.g., He et al., 2021; Zheng et al., 2021). However, the data set is also consistent with an internal paleodrainage, as proposed by Y. Zhang et al. (2019). Furthermore, the similarity between zircon age populations of Gonjo Basin sediments and bedrock data from the east Qiangtang terrane and the modern local Aiyu River cannot exclude the possibility of a southwestern or more locally derived provenance for the Gonjo Basin sediments. Indeed, a locally derived provenance is consistent with the sedimentology and varied paleocurrent directions in the Gonjo Basin (Studnicki-Gizbert et al., 2008; Figure 4). Therefore, the similarity of the Gonjo detrital zircon U–Pb age spectra to downstream basins cannot be used as conclusive evidence for through-flow of major drainage, particularly since downstream basin detritus may also be locally derived (see Section 4).

4. Do Detrital Zircon U-Pb Data From the Jianchuan Basin Record the Drainage Capture of the Greater Paleo-Red River?

The Jianchuan Basin is located just to the south of the First Bend of the Yangtze River (Figure 7) and would have received a provenance signal from southeast Tibet if a Greater paleo-Red River had flowed from eastern Tibet through the Jianchuan Basin into the South China Sea. Based on detrital zircon U–Pb analyses, the basin is debatably considered to either have received sediments from a major river of eastern Tibet which could have been the paleo-upper Yangtze River before it was captured by the paleo-lower Yangtze (e.g., Clift et al., 2020; Feng et al., 2021; Gourbet et al., 2017; He et al., 2021; Yan et al., 2012; Zheng et al., 2021) or the basin sediments may be locally derived (Sun et al., 2020a; Wei et al., 2016; Wissink et al., 2016).

4.1. Geological Setting of the Jianchuan Basin

The Jianchuan Basin is one of the largest Cenozoic basins on the southeast margin of the Tibetan Plateau. It is located in the southwesternmost part of the South China Block and bounded by the Qiaohou thrust fault to the west and the Jianchuan strike-slip fault to the east (Figure 7). The Qiaohou Fault carries Triassic rocks over the Jianchuan Basin and controls the subsidence and folding of the Basin (Cao et al., 2019; Gourbet et al., 2017). Low-temperature thermochronological data suggest that the Qiaohou Fault was active around 50–39 Ma (Cao et al., 2020). To the west of the Jianchuan Basin lies the Lanping-Simao fold belt (Figure 7), the northern extension of the Indochina terrane. The Lanping-Simao fold belt is covered mainly by Mesozoic and early Cenozoic red beds (Figure 7). The Cenozoic Lanping Basin generally has stratigraphy similar to the Jianchuan Basin (Yunnan Bureau of Geology and Mineral Resources (YBGMR), 1990).

4.2. Stratigraphy and Sedimentology of the Jianchuan Basin

A major impediment associated with the comparison and compilation of previous detrital zircon studies in the Jianchuan Basin is the variations in stratigraphies that different researchers have used. We therefore start by reviewing the stratigraphy and sedimentology of the Jianchuan Basin and note the stratigraphic framework adopted in this study (Figure 8).

Based on the geological map of Yunnan Province (YBGMR, 1990), the Jianchuan Basin was previously thought to have accumulated the most continuous sedimentary succession on the southeast margin of Tibet, with a total thickness of more than 6 km. From oldest to youngest, the formations were divided into the Paleocene Yunlong and overlying Guolang formations (sometimes combined as the Mengyejing Formation), the Eocene Baoxiangsi Formation, the Oligocene Jinsichang Formation, the Miocene Shuanghe Formation, and the Pliocene Jianchuan and Sanying Formations (Figure 8a). However, the ages of these formations were based on limited ostracods, charophyte flora, and plant fossils, and were significantly modified in recent years.

Both the Yunlong and Guolang formations mainly consist of red violet, thin-bedded horizontally laminated mudrock and marlstone interbedded with red sandstone, interpreted as fluvial floodplain and lacustrine deposits (Wei et al., 2016). Gourbet et al. (2017) merged the Yunlong and Guolang formations together as the Mengyejing

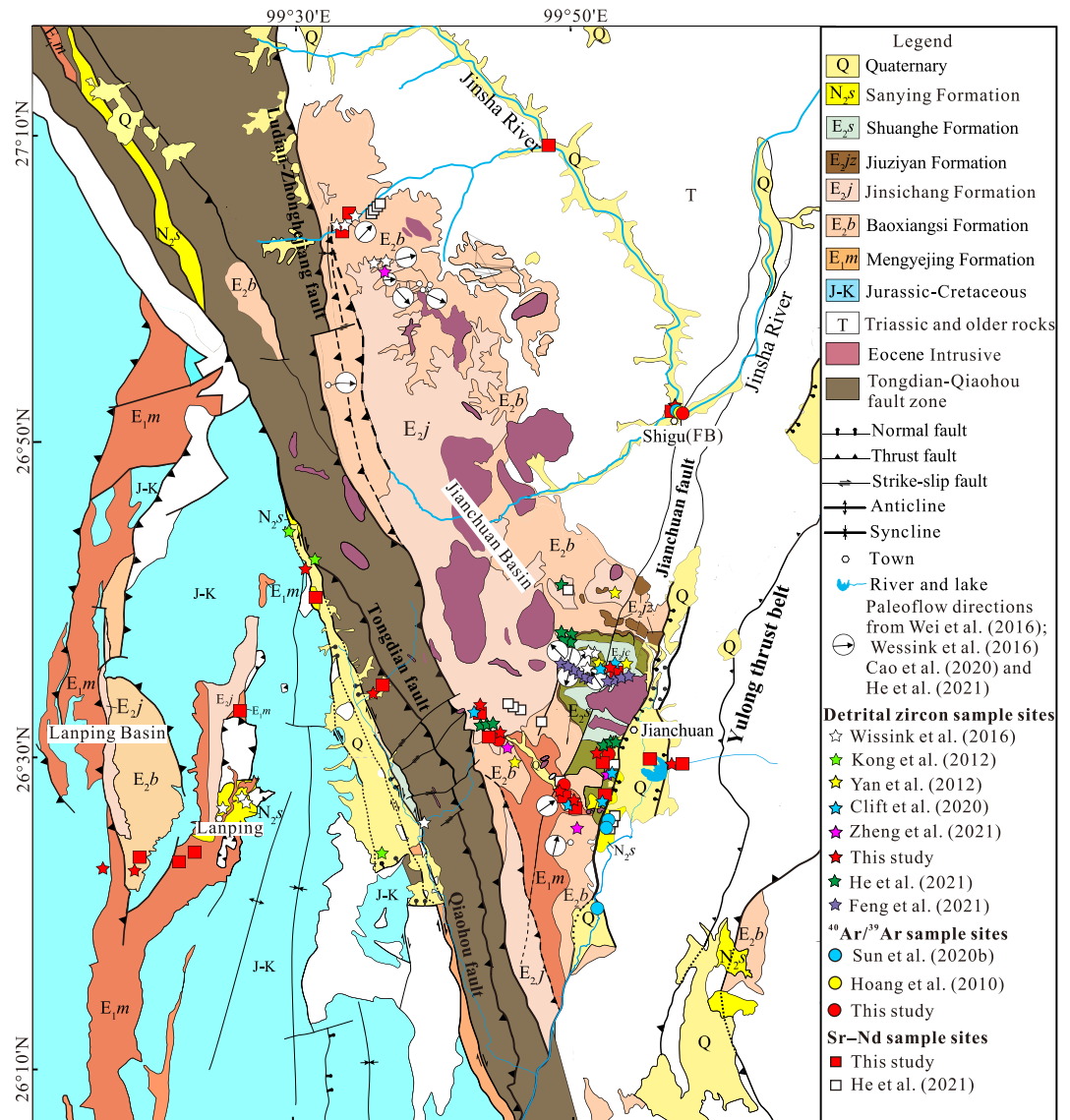


Figure 7. Geological map of the Jianchuan Basin and surrounding area, modified after YBGM (Yunnan Bureau of Geology and Mineral Resources, 1990) and Cao et al. (2021). The sampling locations of detrital zircon U–Pb, ⁴⁰Ar/³⁹Ar, and Sr–Nd in previous work and this study are marked by different symbols. Arrows with circles denote the paleocurrent directions; data are from Wei et al. (2016), Wissink et al. (2016), and He et al. (2021).

Formation and assigned a Paleocene to early Eocene age to it (Figure 8c). However, a recent magnetostratigraphic study in the southern part of the Simao Basin (see Figure 2 for location) suggested that the Mengyejing Formation is Late Cretaceous (~112–63 Ma) (Yan et al., 2021).

The Baoxiangsi Formation consists of massive breccias composed of exclusively angular to subangular, poorly sorted limestone clasts, interbedded with sandstones, conglomerates with basement clasts, and massive red multi-storey sandstones with an abundance of planar cross-bedding, with a total thickness of ~800 m (Figure 8b). The deposits are interpreted as braided fluvial channels with laterally adjacent alluvial fans fed from proximal high relief (Gourbet et al., 2017; Wei et al., 2016). The Jinsichang Formation is mainly comprised of both clast-supported and matrix-supported conglomerates interbedded with coarse sandstones at the bottom, siltstones, mudstones and fine-grained sandstones in the middle, and massive and thick-bedded conglomerates and coarse-grained sandstones at the top (Wei et al., 2016; Figure 8b). The total thickness of the Jinsichang Formation is considered to be more than 2,000 m and interpreted as deposited in a braided fluvial environment. Gourbet et al. (2017) merged the Baoxiangsi and Jinsichang formations, considering them to be lateral facies

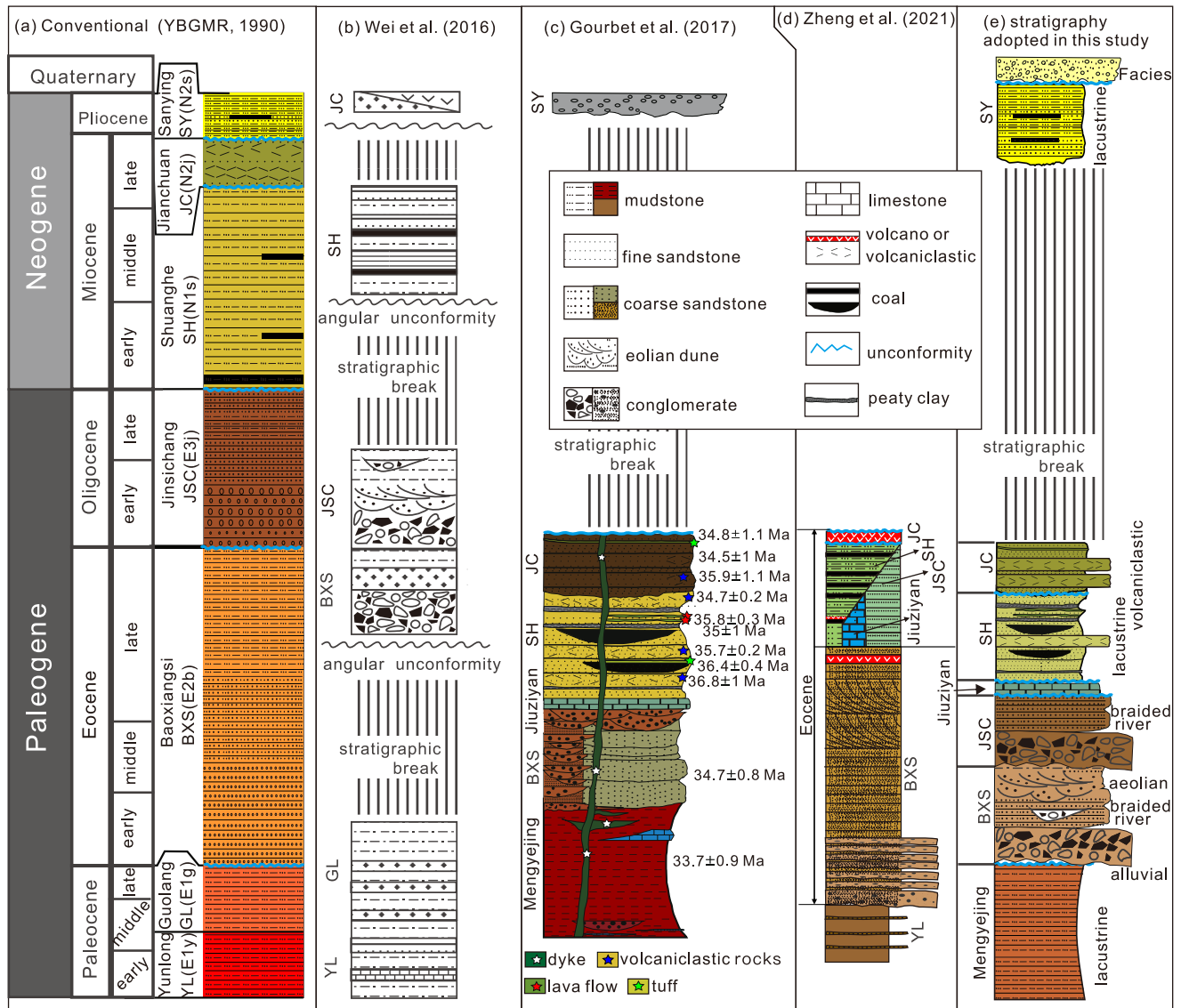


Figure 8. Diagram showing the different proposed stratigraphic frameworks for the Jianchuan Basin. Numerical ages shown in the panel of Gourbet et al. (2017) are from isotopic analyses carried out on various rock types as depicted. In the stratigraphy adopted for this paper (right panel), facies are from Wei et al. (2016) and Gourbet et al. (2017). We retain the individual Eocene formations. We extend the Baoxiangsi Formation into the early Eocene as there is no maximum age constraint. We do not extend the Baoxiangsi Formation into the late Eocene because the overlying Jinsichang and Shuanghe Formations are of this age. However, we acknowledge the argument of Gourbet et al. (2017) that undated syenite cobbles in the Baoxiangsi Formation may come from a local late Eocene syenite, which would indicate that deposition continued until that time.

variations. However, as noted by Wei et al. (2016), the varied lithologies of the Baoxiangsi Formation represent diverse facies associations (Figures 8b and 8c). The breccias are typical debris-flow deposits and the interbedded sandstones represent channel fills. The cross-bedded sandstones of the upper Baoxiangsi Formation were previously considered as evidence of a large river (Clark et al., 2004; Gourbet et al., 2017; Yan et al., 2012; Zheng et al., 2021). However, the surface microscopic characteristics of quartz sand grains and sedimentary structures such as large-scale cross-bedding suggest an aeolian origin for the sandstone in the upper part of the Baoxiangsi Formation (Cui et al., 2011). Moreover, Wei et al. (2016) also noted that the Baoxiangsi Formation displays marked lateral facies variations (Figure 8b), as manifested by distinct facies sequences in different localities. By contrast, the Jinsichang Formation lacks aeolian facies, and the conglomerates and sandstones are best explained as alluvial fan and braided river deposits (Wei et al., 2016). Considering the significantly different lithologies between the Baoxiangsi and Jinsichang Formations, we retain the Baoxiangsi and Jinsichang as separate formations, in agreement with most previous studies (Figure 8c).

Above the Jinsichang Formation, Gourbet et al. (2017) newly identified a ~100 m carbonate succession, which they named as the Jiuziyan Formation. This, and the overlying coal-bearing thinly laminated mudstones, siltstones and fine sandstones of the Shuanghe Formation are interpreted as palustrine-lacustrine deposits (Gourbet et al., 2017). The Shuanghe Formation was originally assigned as Miocene aged based on the well-known “Shuanghe flora” (YBGMR, 1990). The overlying Jianchuan Formation consists of trachyte, volcanic breccias, and tuffs interbedded with volcano-sedimentary and pyroclastic rocks, and was assigned as Late Miocene-early Pliocene (YBGMR, 1990). However, Gourbet et al. (2017) dated a number of lava flows and cross-cutting igneous rocks from the Jinsichang and Shuanghe formations and showed that both formations are Late Eocene rather than Miocene and Pliocene, as previously suggested (Figure 8c). Zheng et al. (2021) proposed that the Jinsichang, Jiuziyan, and Shuanghe formations are coeval lateral facies variations (Figure 8d), but no evidence was provided. Therefore, we keep the Jinsichang, Jiuziyan, and Shuanghe formations as separate stratigraphic units following most previous studies (Figure 8e).

The Sanying Formation is developed only in the southeastern corner of the Jianchuan Basin (Figure 7). It is mainly comprised of gray and yellow mudstone, interbedded with yellow sandstone and black-greyish lignite (Wang et al., 1998), consistent with deposition in swamp and lacustrine environments. A magnetostratigraphic study suggests a late Miocene-Pleistocene age for the Sanying Formation (Li et al., 2013). Therefore, there are no Oligocene-middle Miocene sediments in the Jianchuan Basin.

4.3. Provenance of the Jianchuan Basin Based on Detrital Zircon U–Pb Ages

Previous work utilizing detrital zircon U–Pb data from the sediments of the Jianchuan Basin (Figures 9–12) have suggested that they are either locally derived (Wissink et al., 2016) or that they contribute to evidence that a major river once flowed from SE Tibet to the South China Sea (e.g., Clift et al., 2020; He et al., 2021), and was captured by the paleo-lower Yangtze in the late Eocene (e.g., Feng et al., 2021; Gourbet et al., 2017), Oligocene (Yan et al., 2012), or as late as the Quaternary (Kong et al., 2012).

Yan et al. (2012) carried out the first U–Pb detrital zircon study in the Jianchuan Basin. They considered that the zircon U–Pb age spectrum from their sample from the braided fluvial facies of the Baoxiangsi Formation (sample JSJ15, Figure 9a) looked more similar to the spectrum from the Songpan-Ganzi terrane (see Figure 3) compared to the sample from the modern Yangtze River First Bend (Figure 13d, sample from Hoang et al., 2009). They therefore interpreted the Baoxiangsi Formation to be the result of deposition from a major Songpan-Ganzi draining river, rather than the paleo-upper Yangtze draining the Qiangtang terrane. Yan et al. (2012) considered that this major river ceased flowing through the basin after the deposition of the Baoxiangsi Formation, as evidenced by the first record of a more restricted zircon age spectrum, indicative of local drainage, in the Jinsichang Formation above the Baoxiangsi Formation (sample JSJ18, Figure 10a), although the precise location of this sample in relation to its stratigraphic position is uncertain.

Later workers, for example, Clift et al. (2020), Zheng et al. (2021), He et al. (2021), and Feng et al. (2021) also concurred with the view that the spectra became more restricted after the deposition of the Baoxiangsi Formation. However, they did not make a distinction in terms of whether the Baoxiangsi Formation resembled more the Songpan-Ganzi terrane or a paleo-upper Yangtze River. Instead, they considered that the similarity of the Baoxiangsi Formation to both the Songpan-Ganzi and upper Jinsha signatures as well as to the Gonjo Basin sediments (Section 3.2) indicated that the paleo-upper Yangtze used to flow from eastern Tibet through both these basins. In a variant to this view, He et al. (2021) coupled the zircon U–Pb data with geochemistry and heavy mineral data to show that the Jinsichang Formation was more mineralogically mature compared to the Baoxiangsi and Shuanghe Formations. They therefore considered that the Jinsichang Formation represented the paleo-upper Yangtze, whereas the Baoxiangsi and Shuanghe Formations had greater contributions from local proximal sources. Kong et al. (2012), however, carried out a U–Pb detrital zircon study on the Quaternary sediments (Figure 14b) along the Qiaohou Fault (Figure 7). They found that the U–Pb age spectra of these Quaternary sediments are also similar to the Songpan-Ganzi terrane (Figures 14 and 15a), and therefore concluded that a paleo-upper Yangtze drained from southeast Tibet and connected to the Red River through the Jianchuan Basin throughout the Cenozoic until it was captured by the lower Yangtze at 1.7 Ma.

Wissink et al. (2016) conducted a more comprehensive detrital zircon U–Pb study on the Cenozoic sediments from the southeast margin of Tibet, mainly from the Jianchuan and Lanping basins. By comparing the U–Pb ages of all the Cenozoic samples with the potential bedrock sources, they concluded that the provenance of these Cenozoic sediments can be best explained by local derivation, and therefore did not support a connection between the

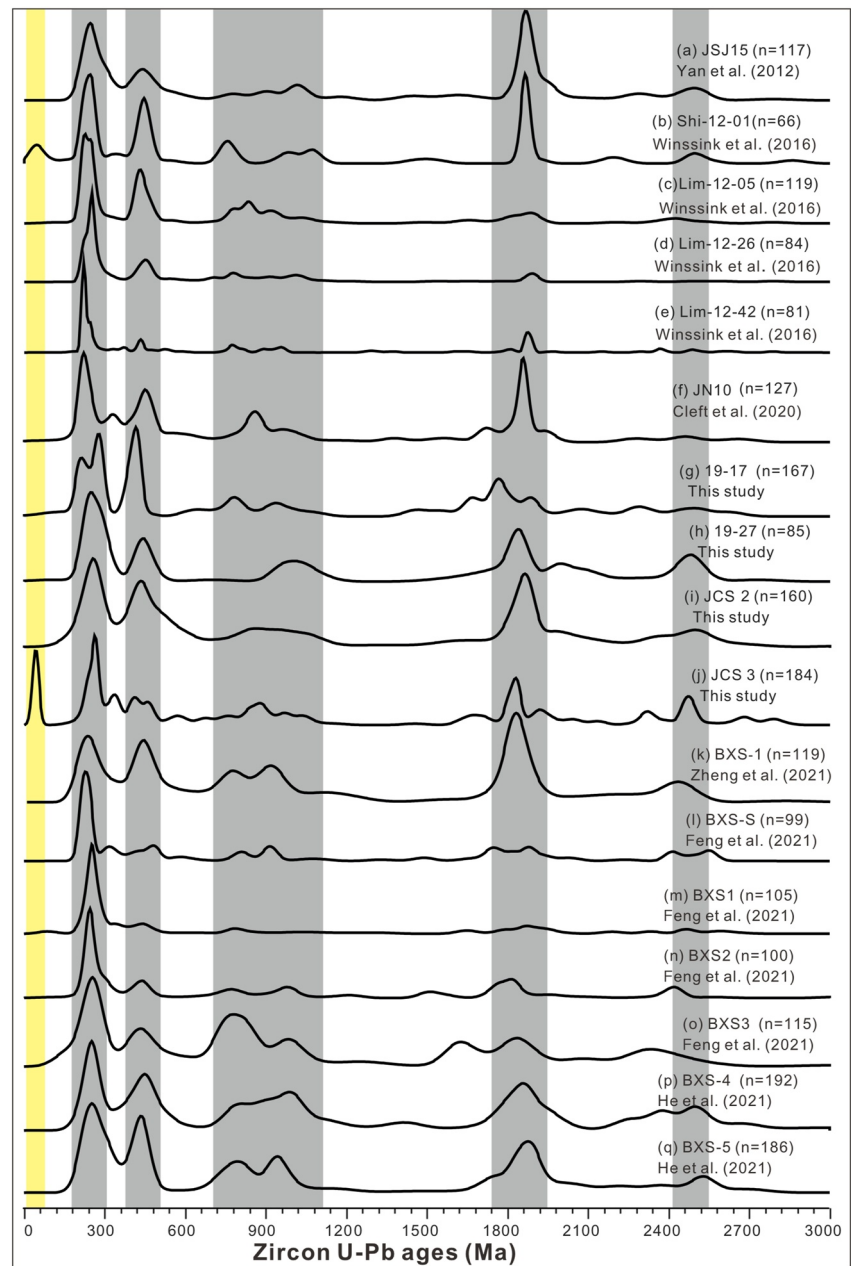


Figure 9. KDE plots of the detrital zircon U–Pb ages from individual samples of the Baoxiangsi formation in the Jianchuan Basin from previous work and this study. The published data are from Yan et al. (2012), Kong et al. (2012), Winssink et al. (2016), Clift et al. (2020), Zheng et al. (2021), He et al. (2021), and Feng et al. (2021). The five vertical bars indicate the common zircon populations in East Asia, as stated in Figure 3. The yellow vertical bar indicates the Cenozoic zircon populations that may be derived from the volcanic rocks in the Jianchuan basin.

paleo-upper/middle Yangtze and paleo-Red River. However, Gourbet et al. (2017) reconsidered the data from the Jianchuan Basin of Winssink et al. (2016) in the light of their new stratigraphy of the basin. They argued that five samples of Winssink et al. (2016) from the upper Baoxiangsi Formation were actually deposited after the time of drainage change from a major through-flowing river to local input as proposed by Yan et al. (2012), while the remaining three samples belonging to the Baoxiangsi Formation have comparable age spectra to those of Yan et al. (2012) (sample JSJ15, Figure 9a), and therefore were also sourced from the Songpan-Ganzi terrane. They concluded that the massive sandstones of the Baoxiangsi Formation correspond to a major river draining the Songpan-Ganzi, which connected a paleo-upper Yangtze with the Red River. They suggested, based on sedimentological evidence, that this major river system was abandoned by the time of deposition of the lacustrine Shuanghe Formation.

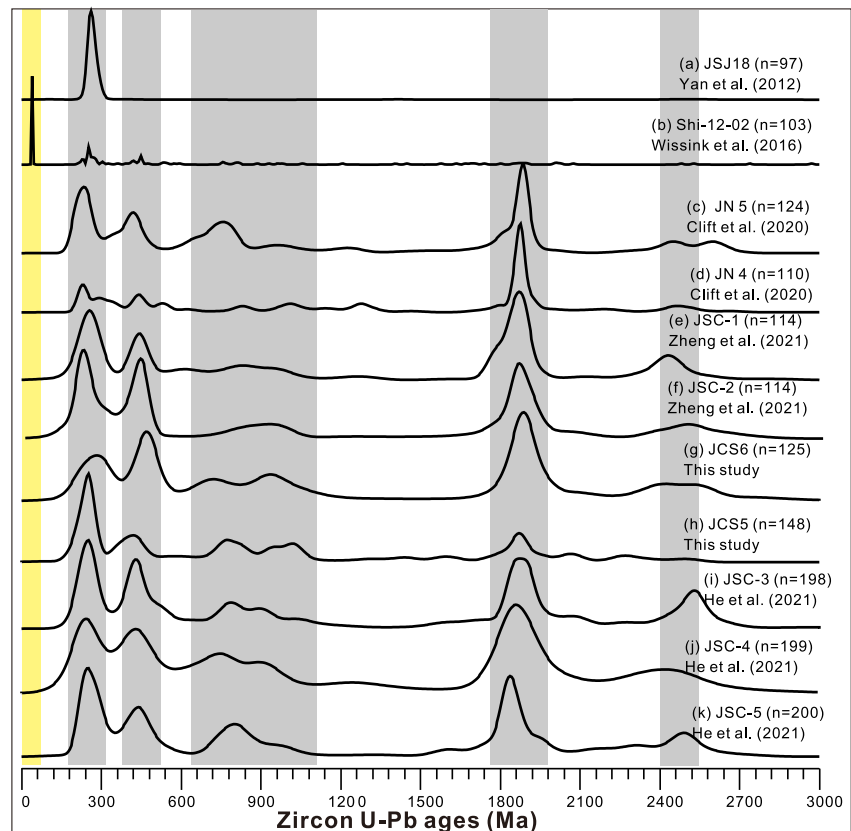


Figure 10. KDE plots of the detrital zircon U–Pb ages from individual samples of the Jinsichang Formation in the Jianchuan Basin from previous work and this study. The vertical bars are the same as Figure 9.

From the above, we note that there are three main questions with respect to the provenance of the sediments in the Jianchuan Basin:

First, is the Baoxiangsi Formation detrital zircon spectrum sufficiently similar to the Songpan-Ganzi terrane and dissimilar to the Yangtze First Bend sediments to conclude that the Formation does not represent the paleo-upper Yangtze, as Yan et al. (2012) proposed?

Second, do the formations younger than the Baoxiangsi Formation record significant provenance changes due to river capture? Or alternatively, could they still be considered as trunk river sediments, as for example, proposed by He et al. (2021), with some previously analyzed samples representing local input that may not represent the dominant facies?

Third, could the Jianchuan basin sediments be locally derived, as Wissink et al. (2016) proposed?

In order to elucidate the three questions posed above, we collected 10 samples for U–Pb detrital zircon analysis: four from the Baoxiangsi Formation, two from the Jinsichang Formation, two from the Shuanghe Formation, and one from each of the Jianchuan and Sanying Formations. We also collected samples from the Late Cretaceous bedrock close to the Jianchuan Basin and modern river sediments at the Yangtze first bend as well as local rivers in the Jianchuan Basin to assess the possibility of locally derived provenance (Figure 7, see Table S2 in Supporting Information S2 for sample details). Furthermore, we compiled all the previously published detrital zircon U–Pb data from the Jianchuan Basin (Table S4 in Supporting Information S2), as shown in Figures 9–12. We use the updated stratigraphic framework based on recent new age constraints (see Section 4.2 and Figure 8) for each sample location.

From our compilation, we address the above three questions as follows:

- (1) Using visual comparison of the KDE plots (Figure 14), with the acquisition of more data, the spectra from the Songpan-Ganzi and the Yangtze First Bend are insufficiently different from each other to be able to deter-

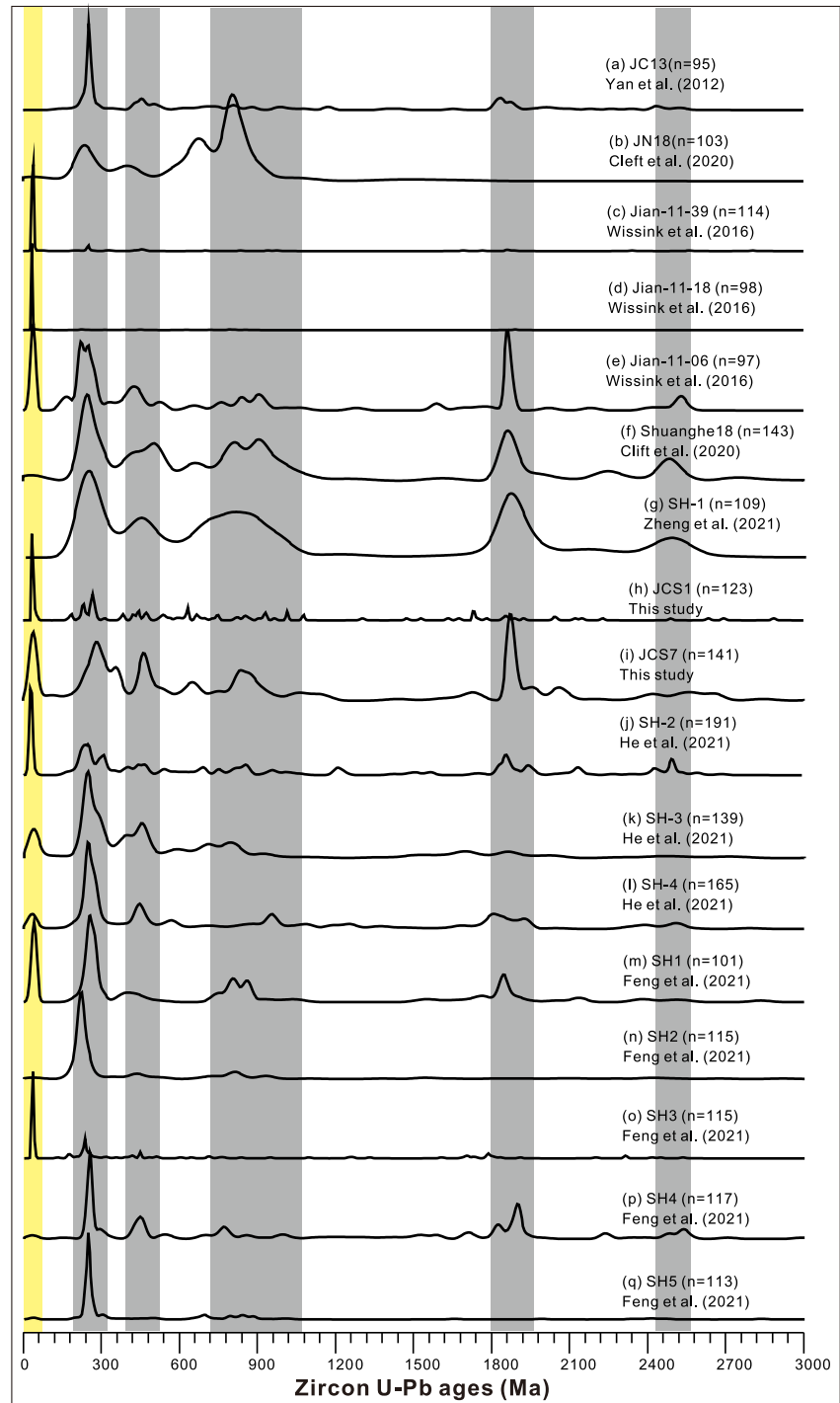


Figure 11. KDE plots of the detrital zircon U-Pb ages from individual samples of the Shuanghe Formation in the Jianchuan Basin from previous work and this study. The vertical bars are the same as Figure 9.

mine whether the Baoliangsi Formation was derived from one or the other. Specifically, the criteria that Yan et al. (2012) used, namely that the Baoliangsi Formation matches closely with the Songpan-Ganzi spectrum particularly in terms of a pronounced peak at 1.8–2.0 Ga and differs from the Yangtze First Bend spectra in terms of the Baoliangsi Formation lacking Neo- and Meso-Proterozoic grains in the range 1.4–1.8 Ga and 600–1,000 Ma, is not upheld. Figure 14h shows that the Baoliangsi Formation does have a considerable number of such Neo- and Meso-Proterozoic grains, whilst the more diffuse nature of the 1.6–2.0 Ga peak of

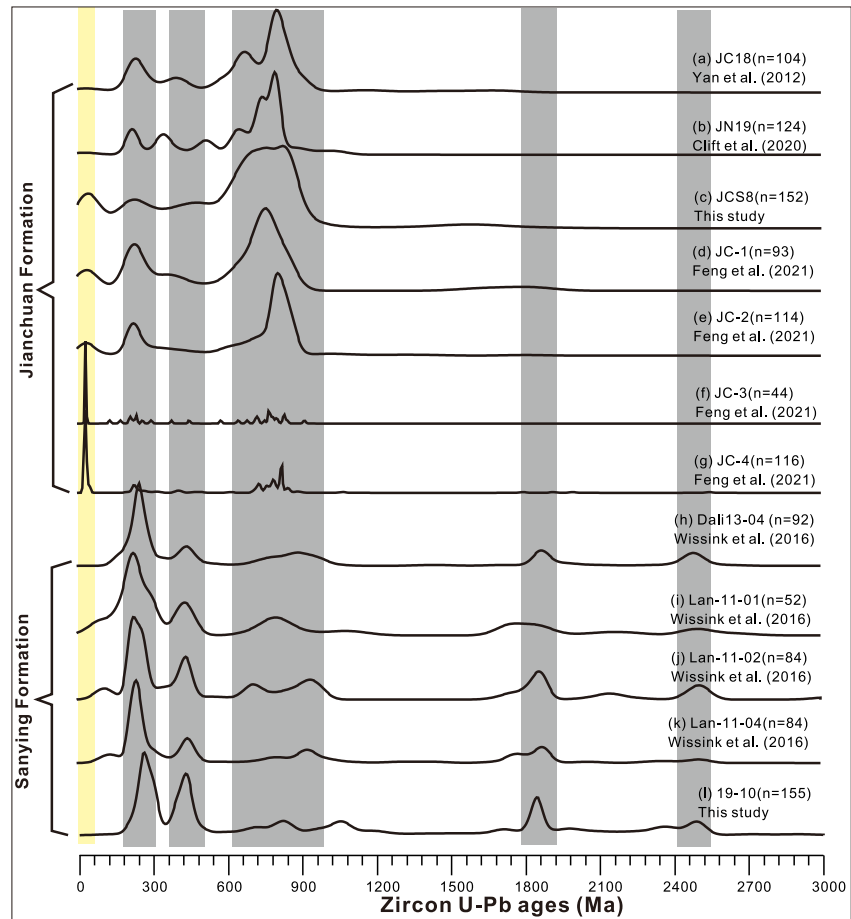


Figure 12. KDE plots of the detrital zircon U–Pb ages from individual samples of the Jianchuan and Sanying formations in the Jianchuan Basin from previous work and this study. The vertical bars are the same as Figure 9.

the Yangtze First Bend (Figure 14a) compared to the 1.8–2.0 Ga pronounced peak of the Baoxiangsi Formations and Songpan-Ganzi (Figures 14h and 14k), is not entirely diagnostic. Similarly, the observation that the Baoxiangsi Formation more closely resembles the Songpan-Ganzi terrane rather than the paleo-upper Yangtze in its lack of Cenozoic young ages (P. Zhang et al., 2019) is obviated by new samples from the Baoxiangsi Formation from which young grains are recorded (e.g., Figure 9j). The discovery of these young ages does not mean, however, that the Baoxiangsi Formation is more likely derived from the paleo-upper Yangtze, since young volcanic rocks are also prevalent in the Jianchuan Basin (Figure 7).

Using the MDS plot to determine the degree of similarity between samples (Figure 15) shows that the Baoxiangsi Formation is similar to both the Songpan-Ganzi terrane and Upper Yangtze First Bend end members, and therefore could be equally well derived from either. Therefore, in summary, the original proposal by Yan et al. (2012) that the Baoxiangsi Formation sediments were deposited by a major river draining the Songpan-Ganzi, which was not the paleo-upper Yangtze, is not upheld with the subsequent inclusion of additional data.

- (2) A number of previous authors proposed river capture by the time of deposition of the Jinsichang or Shuanghe Formation, based on sedimentological facies criteria (e.g., Gourbet et al., 2017) and the more restricted zircon spectra (e.g., Feng et al., 2021; Yan et al., 2012). However, as already noted by Clift et al. (2020) and Zheng et al. (2021), their four samples from the Jinsichang Formation (JN4 and JN5 from Clift et al. (2020) and JCS-1 and JCS-2 from Zheng et al. (2021); Figures 10c–10f) as well as our two new samples from this formation (JCS5 and JCS6, Figures 10g and 10h), show broad zircon age spectra, with very similar age distributions and position on the MDS plot to those of the Baoxiangsi Formation (Figure 15b). This mix of

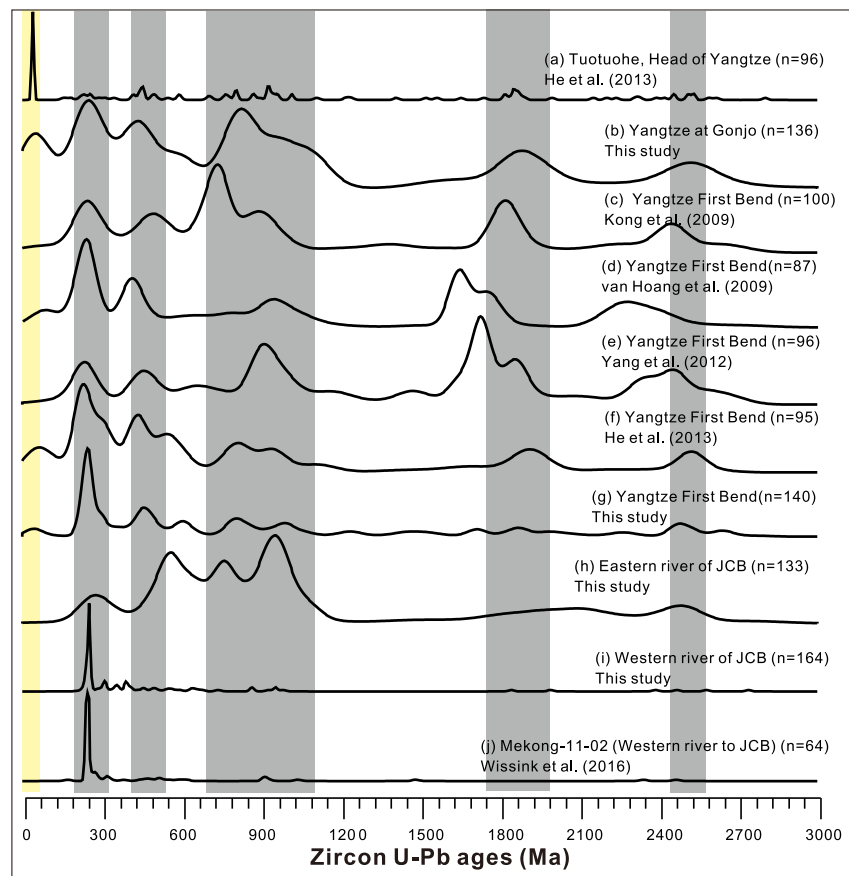


Figure 13. KDE plots of the detrital zircon U–Pb ages from modern Yangtze River samples at Tuotuohe (a, head of the Yangtze, He et al., 2013), at Gonjo (b, this study), and at the First Bend of Yangtze (c–g), as well as local rivers draining in to Jianchuan Basin (h–j). The vertical bars are the same as Figure 9.

samples with broad and restricted spectra could be indicative of a major river with additional local input and lateral facies variation, as proposed by He et al. (2021).

The Shuanghe Formation has a significant proportion of Cenozoic zircon U–Pb ages, resulting in it looking considerably different from the other formations (Figure 14f) and distinct on the MDS (Figure 15a). However, after excluding grains <60 Ma, the Shuanghe Formation signature is closer to the Baoxiangsi and Jinsichang formations, as shown both in KDE and MDS plots (Figures 14e and 15b). Thus, this formation could still represent a major river, with additional significant input of Cenozoic volcanic zircons derived from local Jianchuan volcanic rocks of this age (see Figure 7). Furthermore, a number of samples from the Shuanghe Formation overlap with those from the Baoxiangsi and Jinsichang Formations (Figure 15b), suggesting the possibility that the various samples represent a combination of facies from a through-going river and locally derived deposition.

The only exception to the similar spectra in the formations of the Jianchuan Basin sediments is found in the Jianchuan Formation. In this formation, all the samples have simple age spectra (Figure 14d) and are dominated by Cenozoic and 600–900 Ma age populations. The Cenozoic grains may well be derived from the local Jianchuan volcanics such as the Shuanghe Formation, whereas the 600–900 Ma age populations are most likely transported by the local eastern river draining from the Yangtze Block into the basin today, which is also dominated by a Neo-Proterozoic age spectrum (Figure 13h, eastern river to JCB).

Therefore, in summary, the detrital zircon U–Pb data do not rule out that a major river continued to flow through the region until the Jianchuan Formation time. There is no abrupt change of provenance in the Jianchuan Basin between the Baoxiangsi, Jinsichang, and Shuanghe formations, reflecting the time of river capture when facies changed from a major river to local inputs. Instead, the signature which

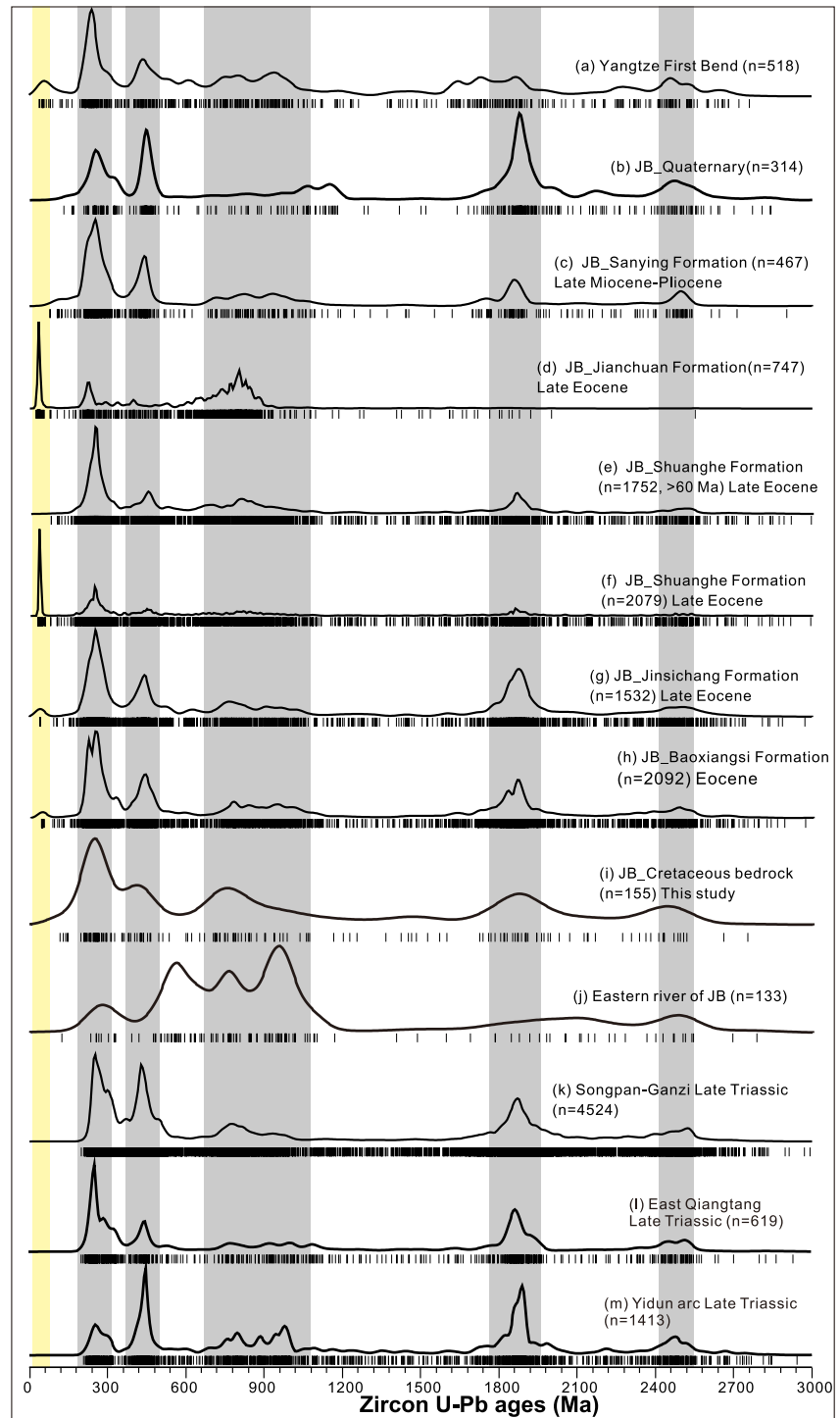


Figure 14. KDE plots of detrital zircon U-Pb ages, combining all samples for each formation in the Jianchuan Basin (b–h) and comparisons with the Yangtze First Bend (YZ_FB, a), Cretaceous sedimentary bedrocks around the Jianchuan Basin (i), a local river from the eastern side of the Jianchuan Basin (j), and Late Triassic sedimentary bedrocks from Songpan-Ganzi (k), Yidun Arc (l) and Qiangtang (n) terranes. The vertical bars are the same as Figure 9.

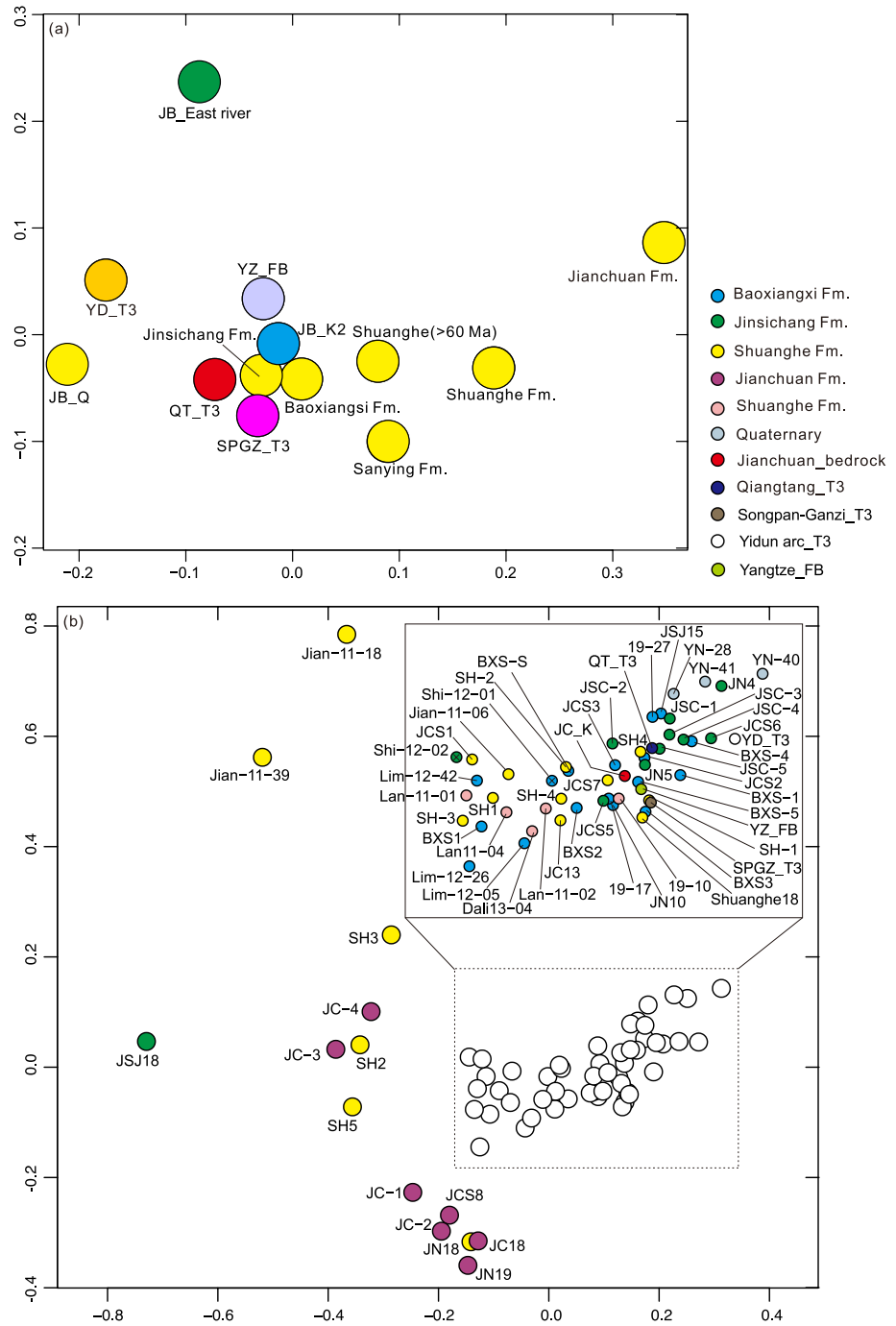


Figure 15. (a) MDS plot using the data of Figure 14. (b) MDS plot using all the individual samples from the Jianchuan Basin, data from Figures 9–12. The inset box represents an enlarged view of the dashed area. The two Baoxiangsi and Jinsichang Formation samples interpreted by Wissink et al. (2016) as transverse fluvial facies are depicted by a cross through the symbols. T2 = Mid Triassic, T3 = Late Triassic, J1, 2 and 3 = Early, Middle, and Late Jurassic, K1 and 2 = Early and Late Cretaceous, Pg = Paleogene, Mio = Miocene, Plio = Pliocene, Q = Quaternary.

previously has been interpreted as that of a major river, continues in some samples until the Pliocene or as late as Quaternary (Figure 14b). Previously documented provenance changes may reflect only that samples were collected from different facies in an intermontane basin, rather than upstream river capture.

- (3) Both the KDE plots and the MDS plots show that the detrital zircon U–Pb spectra from the Baoxiangsi Formation, Jinsichang Formation, and Shuanghe Formation (excluding grains <60 Ma) look equally similar to the Yangtze First Bend and the local Cretaceous bedrock (Figures 14 and 15), indicating that a local derivation could well explain the major Jianchuan basin sediments, as proposed by Wissink et al. (2016). The significant young Cenozoic grains from the sediments of the Jianchuan Basin may suggest a source from the Qamdo Block, as Clift et al. (2020) suggested. However, these young grains could also be locally derived, as shown by the widespread Cenozoic igneous rocks in the Jianchuan Basin. Therefore, long-distance transport of these young grains from the Qamdo Block is not required. Overall, we have shown that if one is to investigate if local sourcing could produce the observed age spectra, thus negating the need for long distance transport of detritus, comparison with signatures from local older bedrock and rivers is required.

5. Alternative Provenance Approaches to Investigating River Capture: Evidence From Bulk Sr–Nd Isotope and Mica $^{40}\text{Ar}/^{39}\text{Ar}$ Analyses?

With the challenges of the use of zircon in providing adequately differentiable source characterization, as described above, we carried out a pilot study applying Sr–Nd whole rock and mica $^{40}\text{Ar}/^{39}\text{Ar}$ analyses to rocks of the Gonjo and Jianchuan Basins to test whether they might provide good approaches for source discrimination, and hence paleo-drainage reconstruction in this region. Our rationale was that, rather than focusing on geological events associated with crystallization (i.e., zircon U–Pb analyses), an approach that focused on the timing of cooling of terranes (as determined from mica $^{40}\text{Ar}/^{39}\text{Ar}$ dating) or distinctive composition of the source rock and the age of crustal material (as determined by Sr–Nd isotopes on bulk rocks), might provide better discrimination between sources.

Although Clift (2016) suggested that both Sr–Nd isotopes and mica $^{40}\text{Ar}/^{39}\text{Ar}$ ages have many uncertainties as provenance tools in SE Asia, some previous studies have proposed successfully constraining the capture history of the Greater paleo-Red River and paleo-Yangtze River using these techniques. For example, Hoang et al. (2010) noted a contrast in $^{40}\text{Ar}/^{39}\text{Ar}$ mica ages between the First Bend of the Yangtze (see Figure 16 for location (Triassic-dominated population, Figure 17v)) and the Red River upper reaches (Cenozoic-dominated population, Figures 17o–17q), and therefore considered that “this method is a good proxy for reconstructing sediment provenance of the Greater paleo-Red River system.” Furthermore, Sun et al. (2020b) compared detrital zircon U–Pb ages and detrital mica $^{40}\text{Ar}/^{39}\text{Ar}$ ages from the modern Yangtze River drainage basin and demonstrated that different provenance information is provided by these contrasting systems. In particular, they noted that the Dadu tributary to the Min River (see Figure 16 for location) contains a Cenozoic mica population that may be diagnostic of the paleo-upper Yangtze (Figure 17s), allowing them to constrain aspects of the capture history by comparison with ancient deposits downstream (Sun et al., 2017, 2021). Additionally, they considered micas from Pliocene sediments in the Jianchuan Basin to be locally derived, thereby constraining the time the Yangtze flowed through the basin as pre-Pliocene (Sun et al., 2020c). Clift, Blusztajn, and Duc (2006) conducted Sr–Nd analyses on mudstones from the Hanoi Basin at the Red River mouth (see Figure 16 for location), which showed a rapid shift to less negative ϵNd values at late Oligocene–early Miocene times (Figure 18a). They attributed this shift to be the result of the loss of the paleo-middle Yangtze that flowed from the ancient Yangtze craton into the paleo-Red River basin. Although P. Zhang et al. (2019) noted that the shift in ϵNd values may have a much more complex cause, nevertheless, they still considered that the provenance change recorded by Sr–Nd from the Hanoi Basin is “the strongest line of evidence to date” to support a river reorganization of the Greater paleo-Red River.

5.1. $^{40}\text{Ar}/^{39}\text{Ar}$ Dating of Detrital Micas as a Tool for Reconstructing the Paleodrainage of the Region

Two main strands of research have been undertaken on this topic using detrital mica $^{40}\text{Ar}/^{39}\text{Ar}$ analyses; one strand has looked at using mica $^{40}\text{Ar}/^{39}\text{Ar}$ analyses to determine if and when the paleo-upper Yangtze used to drain into the paleo-Red River using the Greater paleo-Red River sediments (Hoang et al., 2010; Sun et al., 2020c), whereas the second strand of research looked at the time when the Yangtze established its current drainage pattern, using paleo-lower Yangtze sediments (Sun et al., 2017, 2021).

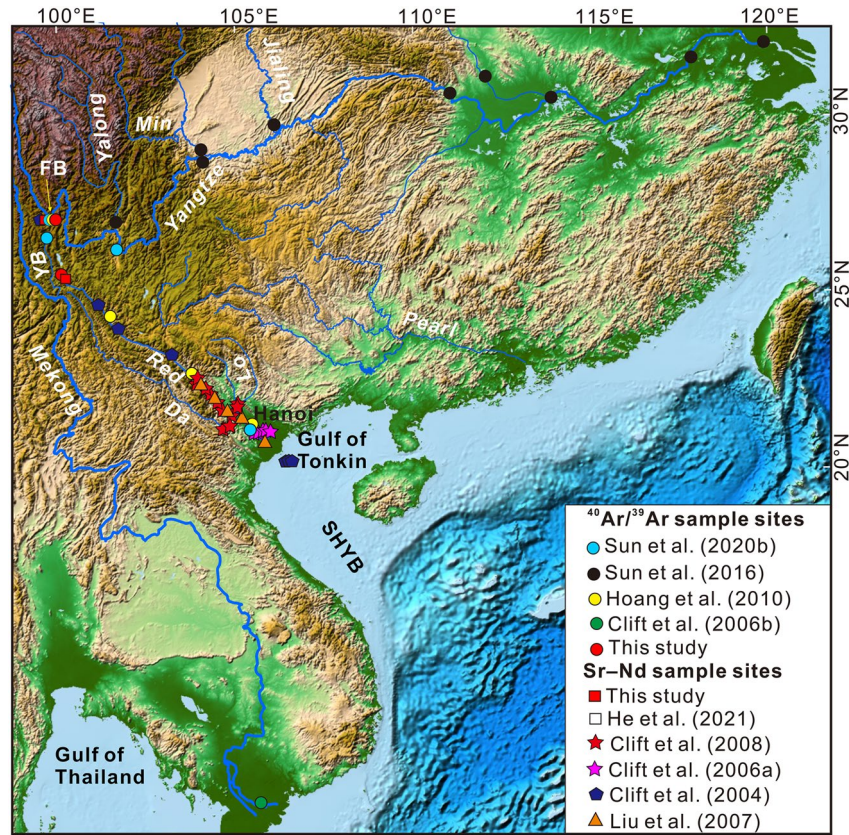


Figure 16. Map showing the sampling locations for mica $^{40}\text{Ar}/^{39}\text{Ar}$ and Sr-Nd bulk sample analyses from modern rivers analyzed in previous published research and this study. Note that whilst the modern upper Yangtze is defined as the region upstream of the Three Gorges, the paleo upper Yangtze is defined by Clark et al. (2004) as upstream of the First Bend, with the paleo middle Yangtze flowing between the First Bend and the Three Gorges—see Figure 2.

5.1.1. Did the Paleo-Upper Yangtze Once Flow Into the Paleo-Red River, as Evidenced by Mica $^{40}\text{Ar}/^{39}\text{Ar}$ Data?

Given the proposal by Hoang et al. (2010) that mica $^{40}\text{Ar}/^{39}\text{Ar}$ ages could be a good tool for detecting river capture using contrasting Triassic and Cenozoic ages from the upper Yangtze and Red River, respectively (see above), we undertook additional analyses at the First Bend of the Yangtze and the Red River head (see Figure 16 for location) to further test this approach (the methods and results of the $^{40}\text{Ar}/^{39}\text{Ar}$ mica analyses are provided in Text S2 in Supporting Information S1 and Table S5 in Supporting Information S2, respectively).

Our new analyses from the Yangtze First Bend concur with Hoang et al. (2010) and Sun et al. (2020c), who show an overwhelming Triassic signal at this location (Figure 17v). However, our data from the Red River head also show an overwhelming Triassic population (Figure 17n), compared to the Cenozoic signal at locations further downstream (Figures 17o–17q), the latter presumably more influenced by input from the Cenozoic Ailao Shan-Red River Fault Zone (Clift et al., 2008). The Red River contains both Cenozoic and Triassic populations at its mouth (Figure 17q). This suggests an additional input of a Triassic signal source to the lower stream of the Red River. Given that the Min River tributary to the paleo-middle Yangtze also shows a strong Cenozoic mica peak (Figure 17s) and is also considered to have flowed into the paleo-Red River in pre-capture times (Clark et al., 2004; Figure 2), provenance discrimination and thus constraint to capture models based on “Triassic” versus “Cenozoic” diagnostic mica ages are likely more complicated than originally thought.

Sun et al. (2020c) carried out $^{40}\text{Ar}/^{39}\text{Ar}$ dating and geochemistry of detrital micas in Pliocene sediments from the Jianchuan and Yuanmou basins on the SE margin of Tibet (see Figure 2 for location), both of which are considered to be regions through which a paleo- upper and -middle Yangtze may have flowed into the paleo-Red River. They showed that muscovite ages from Pliocene Jianchuan Basin sediments overlapped with both the

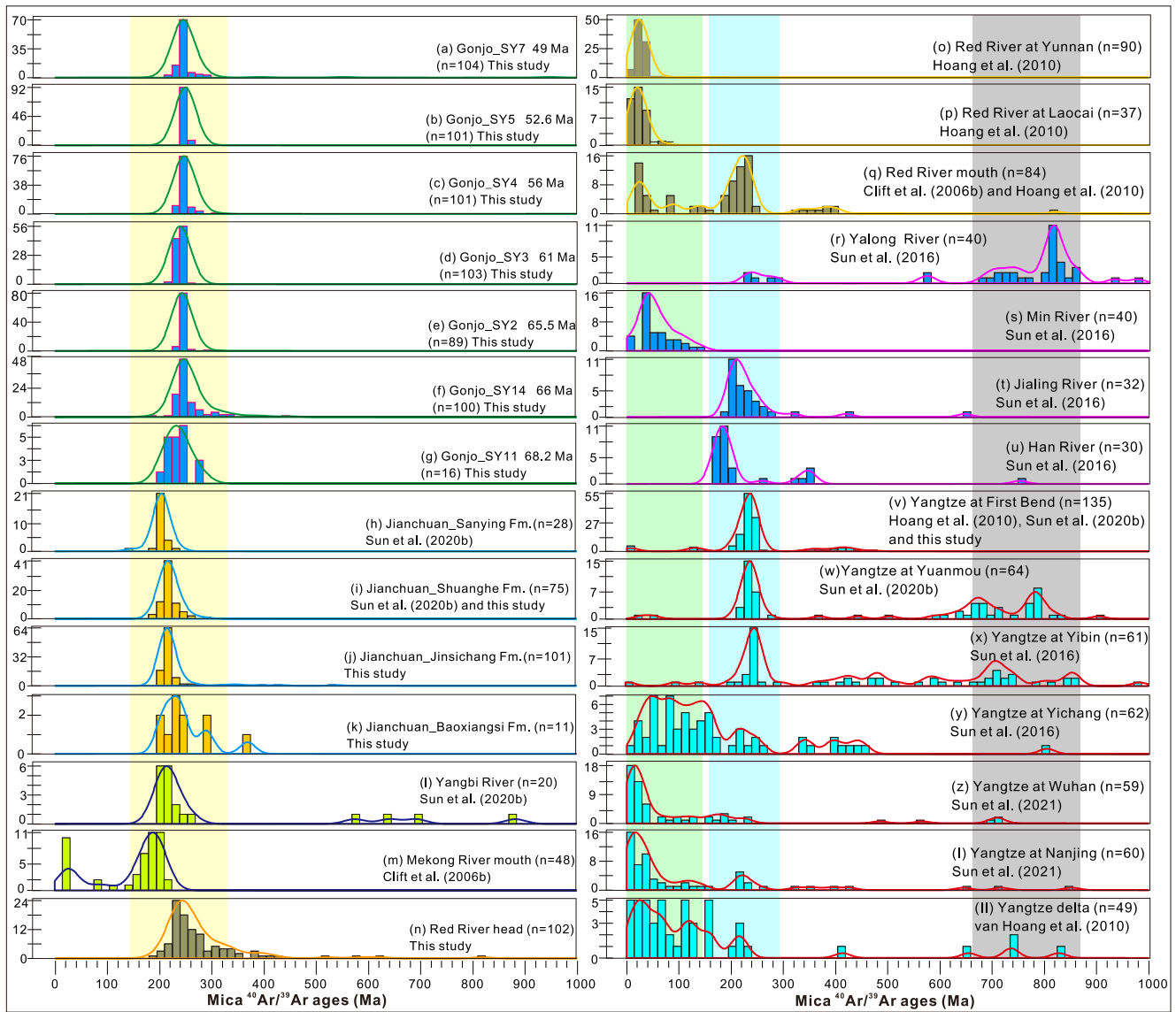


Figure 17. $^{40}\text{Ar}/^{39}\text{Ar}$ ages (as probability density plots) of detrital mica samples from Gonjo Basin (a–g), Jianchuan Basin (h–k), Yangbi river (l), the Mekong River mouth (m), Red Rivers (n–q), tributary rivers of the Yangtze (r–u), and the main Yangtze (v–II).

local Yangbi river that drains the Jianchuan Basin (Figures 17h and 17l) and with the upper Yangtze River, with geochemistry indicating at least some contribution from the upper Yangtze River. By contrast, biotites from the Pliocene Jianchuan Basin sediments had similar ages to a local river draining the basin and a dissimilar signature to the upper Yangtze River. From this, they interpreted that the sediments were recycled from the underlying Eocene Baoxiangsi Formation, which previous provenance studies using zircon U–Pb ages proposed to be deposited by the paleo-upper Yangtze River (see Section 4). They therefore proposed that the paleo-upper Yangtze had ceased draining into the Jianchuan Basin and hence the Greater paleo-Red River prior to the Pliocene.

We note that a requirement for local derivation of the biotite grains does not necessarily require a local source for the muscovite grains, and that the Baoxiangsi Formation may not be derived from the paleo-upper Yangtze (as discussed in Section 4). Since no sediments older than the Pliocene in the proposed paleo-upper Yangtze River drainage basins have been subjected to $^{40}\text{Ar}/^{39}\text{Ar}$ analyses, we collected Paleogene samples from the Gonjo and Jianchuan basins (see Figures 4 and 7 for sampling locations). These can be used to test whether $^{40}\text{Ar}/^{39}\text{Ar}$ muscovite analyses may provide more robust evidence on the evolution of the Greater paleo-Red River and further investigate the potential for the reworking scenario as suggested by detrital zircon U–Pb ages (see Sections 2–4).

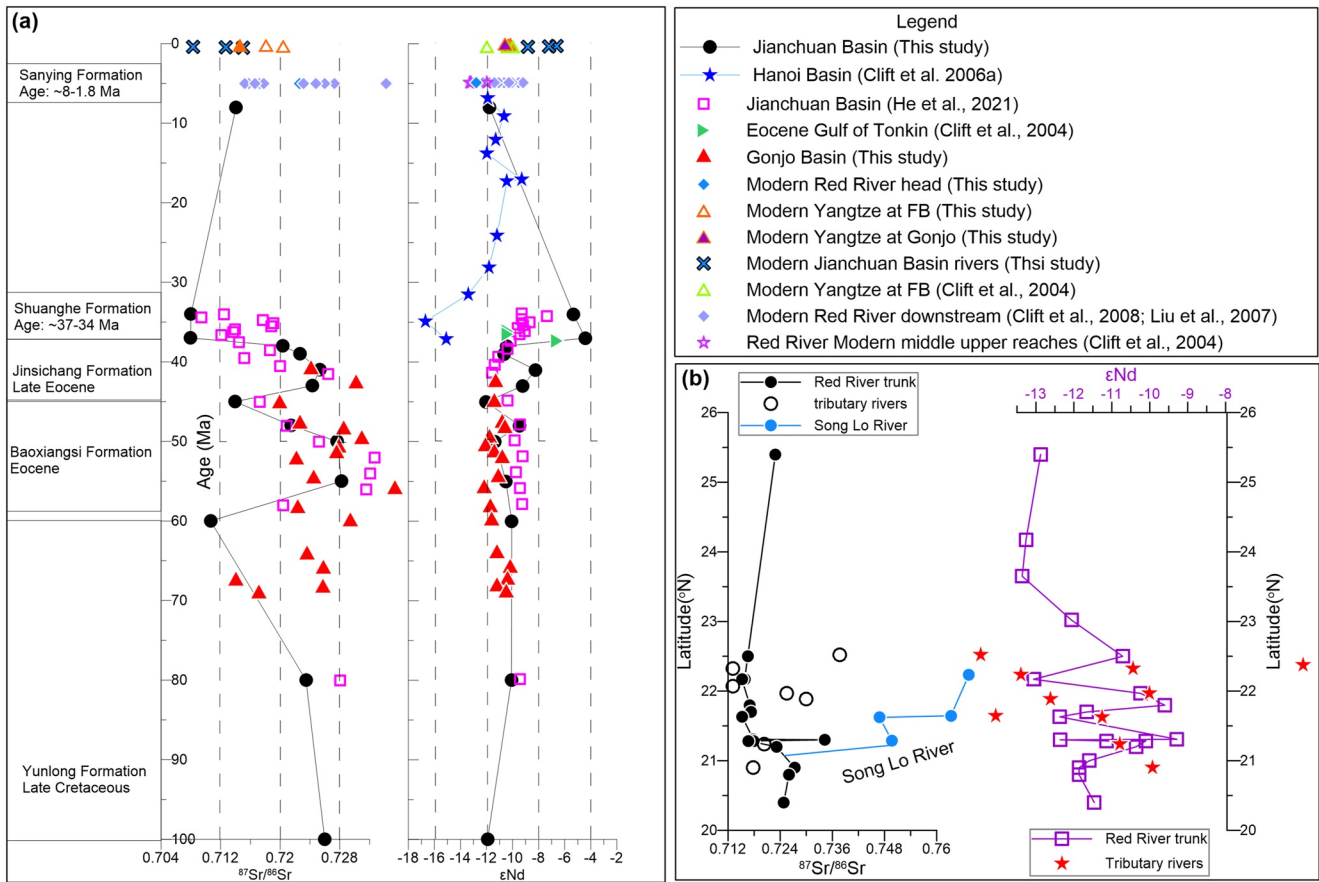


Figure 18. (a) Strontium ($^{87}\text{Sr}/^{86}\text{Sr}$) and neodymium (ϵNd) data from the Jianchuan and Gonjo basins (this study and from He et al. (2021)) compared to previous data from the Hanoi Basin (Clift, Blusztajn, & Duc, 2006; Clift, Carter, et al., 2006), Gulf of Tonkin (Clift et al., 2004), and various modern rivers (data are from Clift et al. (2004, 2008) and Liu et al. (2007)). (b) Diagram showing the downstream variation in $^{87}\text{Sr}/^{86}\text{Sr}$ and ϵNd values from the Red River trunk and its small tributaries.

For the Gonjo Basin, we collected seven samples for $^{40}\text{Ar}/^{39}\text{Ar}$ mica dating spanning the Gonjo Paleogene magnetostratigraphic section (Li, van Hinsbergen, Najman, et al., 2020). For the Jianchuan Basin, we collected nine samples from the Eocene Baoxiangsi Formation, Late Eocene Jinsichang and Shuanghe formations (but only three samples contained micas suitable for $^{40}\text{Ar}/^{39}\text{Ar}$ dating) to complement the Pliocene samples published by Sun et al. (2020c). The methods and results of the $^{40}\text{Ar}/^{39}\text{Ar}$ mica analyses are provided in Text S2 of the Supporting Information S1 and Table S5 in Supporting Information S2.

Plotting our new and compiled data from the Jianchuan and Gonjo basins as KDEs (Figures 17a–17k) and MDS plots (Figure 19), we show that, in both basins, there is little change up section at least since the time of deposition of our oldest sample, with a Triassic age peak dominating throughout, although the Eocene Baoxiangsi Formation has too few data points to allow a robust interpretation. Furthermore, we note that the MDS plot suggests a greater similarity between the Jianchuan Basin sedimentary rocks and the local Yangbi River compared to the Yangtze First Bend, although the number of analyzed mica grains is low for the Yangbi River. Therefore, based on the limited available data, we tentatively concur and extend the interpretation of Sun et al. (2020c) that a local provenance is likely for the Jianchuan Basin, at least since the time of deposition of the Jinsichang Formation. However, we stress that more samples are required from the Jianchuan Basin to validate this interpretation in future studies.

Additionally, our new data from the Paleogene Gonjo Basin (Figures 17a–17g) are similar to the data from the Jianchuan Basin (Figures 17h–17k). This might support the proposal that sediments from both these basins have similar provenance, indicating a through-flowing river, as suggested by previous studies using zircon data (e.g., Clift et al., 2020). However, unfortunately, our analyses from the Baoxiangsi Formation are too few for valid comparison, and furthermore, the sediments from the two basins are not exactly co-eval. We do however note that the Gonjo Basin samples overlap in MDS space with the Yangtze River First Bend, and therefore the Gonjo

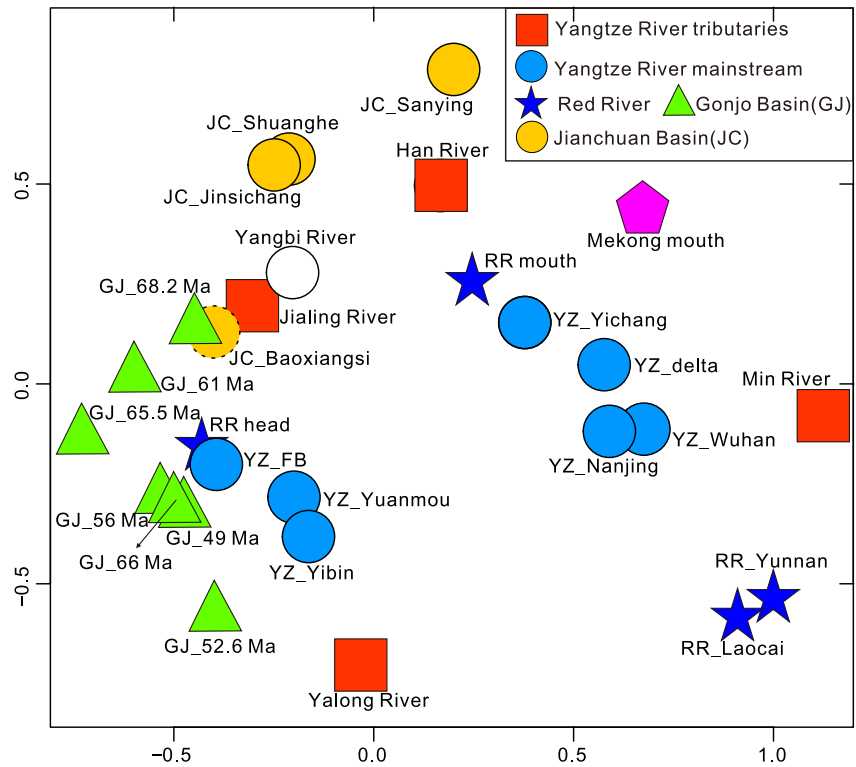


Figure 19. MDS plots of the $^{40}\text{Ar}/^{39}\text{Ar}$ ages in Figure 17. The dashed circle symbol of JC_Baoxiangsi refers to the small number n of analyses from the Baoxiangsi Formation, which makes the data potentially unreliable.

Basin as the headwaters of the paleo-upper Yangtze is viable. Nevertheless, until more samples from local rivers have been analyzed, a local provenance remains equally possible.

5.1.2. When Was the Yangtze River Formed in Its Current Configuration, as Evidenced by Mica $^{40}\text{Ar}/^{39}\text{Ar}$ Data?

Sun et al. (2017) conducted a detrital muscovite $^{40}\text{Ar}/^{39}\text{Ar}$ study on the late Pliocene-Quaternary sediments from the Jiangnan Basin (see Figure 2 for location) through which the modern middle Yangtze flows. They found that the late Pliocene sediments were locally derived, whereas the middle Pleistocene sediments contained a unique Cenozoic age population that could only be sourced from eastern Tibet. They therefore concluded that the paleo-lower Yangtze cut through the Three Gorges (see Figure 2 for location) and reversed the flow direction of the paleo-middle Yangtze between the late Pliocene and middle Pleistocene. They further constrained the lower age limit on the formation of the modern Yangtze by detrital muscovite and K-feldspar dating on the ~Miocene (Zheng et al., 2013) “Yangtze Gravel” of the lower Yangtze at Nanjing (Sun et al., 2021). Since no Cenozoic aged grains from eastern Tibet were identified in the gravel, they therefore concluded that the current Yangtze was established after the Miocene.

In our data compilation (Figure 17), it can be seen that the $^{40}\text{Ar}/^{39}\text{Ar}$ ages along the Yangtze River systematically change from the upper to the lower reaches (see Figure 16 for sampling locations). They are dominated by Triassic ages at the First Bend of the Yangtze (Figure 17v), and there is a significant increase in Neoproterozoic ages after the confluence of the Yalong River to the Yangtze (Figures 17w and 17x); this is consistent with the dominance of Neoproterozoic mica ages in the Yalong River (Figure 17r). The $^{40}\text{Ar}/^{39}\text{Ar}$ ages in the middle and lower reaches of the Yangtze are mainly younger than 120 Ma (Figures 17y and 17z, I, II). These characteristic Cretaceous to Cenozoic ages are predominantly recorded in the Min River tributary to the Yangtze (Figure 17s) and are derived from the Longmen Shan belt (through which the Min River flows (Figure 1)), which has common micas of this age (e.g., Kirby et al., 2002; Wallis et al., 2003). Sun et al. (2017, 2021) considered that the Cenozoic $^{40}\text{Ar}/^{39}\text{Ar}$ ages provide a characteristic signal for the upper Yangtze from eastern Tibet, which can be used

to constrain the formation of the modern Yangtze River. However, the $^{40}\text{Ar}/^{39}\text{Ar}$ ages from the First Bend of the Yangtze (our new data, Hoang et al. (2010), and Sun et al. (2020c); Figure 17v) and Yalong River (Figure 17r) show a paucity of these Cenozoic grains. Therefore, since these Cenozoic micas are only found in the Min River, but not in the trunk stream of the upper Yangtze or the Yalong Rivers from eastern Tibet, the appearance of these grains in the lower Yangtze therefore constrains only when the Min River joined the Yangtze system. The capture of the paleo-middle Yangtze (cut through of the Three Georges) and paleo-upper Yangtze and thus what might be considered the “birth of the Yangtze” remains unknown.

5.2. Sr–Nd Bulk Isotopic Data as a Technique to Determine the Paleodrainage of the Region

Few studies utilizing bulk rock Sr–Nd to investigate paleodrainage in the region have been undertaken so far (Clift, Blusztajn, & Duc, 2006; Clift, Carter, et al., 2006; Clift et al., 2004, 2008; He et al., 2021; Liu et al., 2007), and no unambiguous agreement has been reached. To further explore the significance of these previous studies, we compiled all published data (see Figure 16 for sampling locations), and additionally analyzed bulk mudstones from the Cenozoic Gonjo (18 samples, Figure 4) and Jianchuan (14 samples, Figure 7) basins and river muds from the modern Red and Yangtze Rivers. Methods are given in Text S3 of the Supporting Information S1 and results in Table S6 of the Supporting Information S2 and displayed in Figure 18.

Clift et al. (2004) noted that ϵNd values for the Eocene Red River delta in the Gulf of Tonkin (solid green triangles in Figure 18a) were less negative compared to those of the modern middle upper reaches of the Red River (purple stars), thus requiring that the Eocene material included younger crustal material compared to modern sediment. They proposed two possible interpretations: either the Eocene paleo-Red River included input from the paleo-upper Yangtze, which has modern day values closer to those recorded for the Eocene Gulf of Tonkin (green open triangles in Figure 18a), or there was an additional local contribution from the South China Block to the downstream paleo-Red River record. By contrast, the onshore Hanoi Basin archive of the paleo-Red River shows a major change of ϵNd values from as low as -17 in the Eocene to approximately modern-day values of -11 by the Miocene (Clift, Blusztajn, & Duc, 2006, blue stars in Figure 18a). Clift, Blusztajn, and Duc (2006) interpreted this change to reflect drainage loss of the Greater paleo-Red River by separation from the paleo- upper and -middle Yangtze, which flows over the very negative Yangtze Craton. We suggest that the Gulf of Tonkin data is better explained by additional contribution of material with a less negative ϵNd value to the Red River downstream Hanoi, rather than river capture because (a) the trend to more positive values downstream in the modern Red River (Figure 18b) supports this hypothesis, and (b) the difference in ϵNd values between the co-eval Red River repositories of the onshore Hanoi Basin and off-shore Gulf of Tonkin indicates that an additional source must be supplying the offshore.

The trend to more positive ϵNd values between Eocene and Miocene Hanoi Basin sediments, interpreted as a loss of cratonic input due to capture of the paleo-middle Yangtze away from the Red River (Clift, Blusztajn, & Duc, 2006), seems to provide a more robust argument for river capture. However, as noted by Clift et al. (2008), ϵNd values show strong variations along the trunk of the Red River, and more significant isotopic variability exists in the smaller tributaries, with some extreme values ranging from an ϵNd value of -27 to as high as -6 (Figure 18b). Therefore, we cannot exclude the possibility that the change of ϵNd values in the Hanoi Basin sediments resulted from changes in Red River tributary input.

He et al. (2021) provided Sr–Nd data from Cenozoic sedimentary rocks from the Jianchuan Basin (see Figure 7 for sampling locations), previously interpreted to be either locally derived or the products of a paleo-upper Yangtze draining into the Red River (see Section 4). He et al. (2021) complemented their heavy mineral, bulk geochemical, and detrital zircon data from the Jianchuan Basin with Sr–Nd data. They noted a small excursion to more negative ϵNd values in the Jinsichang Formation compared to the Baoxiangsi and Shuanghe Formations stratigraphically above and below (pink squares in Figure 18a). They considered that this supported their previous interpretation, as constrained by detrital zircon U–Pb data (see Section 4), that a major through-going river of the Greater paleo-Red River developed during the deposition of the Jinsichang Formation. By contrast, our data from the Jinsichang and Shuanghe formations (black solid dots in Figure 18a) show more variability, and indeed some excursion in the opposite direction to that noted by He et al. (2021). We note that the scatter of data within each formation of the Jianchuan Basin (Figure 20-biplot) could be consistent with a mix of local derivation and throughput of a major river as previously proposed (Section 4.3), although the local Jianchuan river signatures are

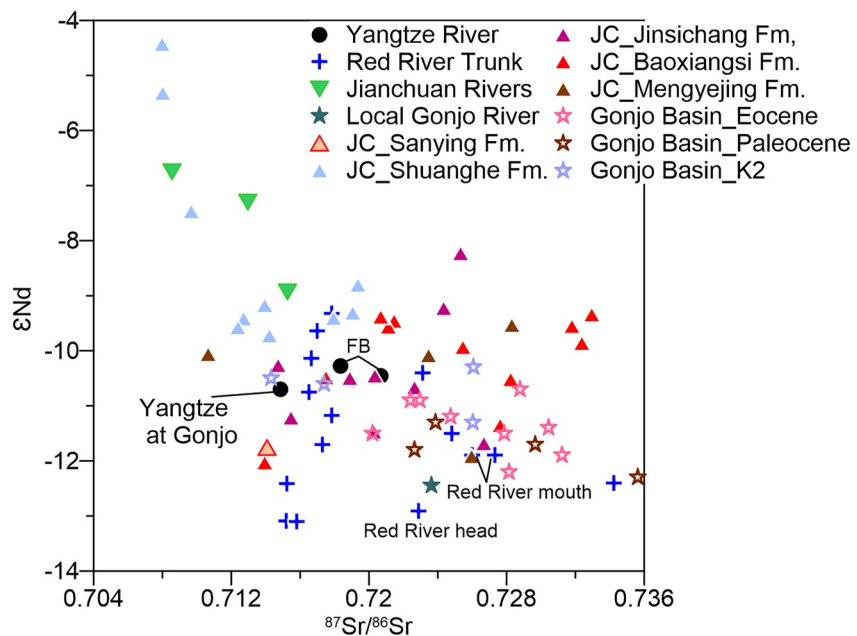


Figure 20. Bi-plot of the strontium ($^{87}\text{Sr}/^{86}\text{Sr}$) and neodymium (ϵNd) data in Figure 18.

dissimilar to the basin's Cenozoic sedimentary rocks, except for the Shuanghe Formation, which can be explained by the high prevalence of contemporaneous volcanic material in this Formation.

He et al. (2021) also compared their detrital zircon data from the Jianchuan Basin with those from the Gonjo Basin, using the degree of similarity to interpret a through-going river between these basins. Comparison of Sr–Nd data for approximately co-eval sediments (the Baoxiangsi Formation in the Jianchuan Basin (pink triangles in Figure 20) and Eocene Gonjo (open pink stars in Figure 20)) between these two basins shows that they plot in broadly different Sr–Nd space albeit with some overlap. This could suggest that, in contrast to the mica (Section 5.1) and zircon data (Sections 3 and 4), the two basins have dissimilar provenance and are not suggestive of a through-going river. Nevertheless, the partial overlap could represent the proposed through-going river, with the non-overlapping samples representing the locally derived facies. We also note that in the Gonjo Basin, the Cenozoic sedimentary rocks are more similar to the modern local Gonjo River compared to the upper Yangtze modern River in the Gonjo region, indicating that a paleo-upper Yangtze is not required to explain the Gonjo Basin data.

6. Discussion

6.1. Implications for the Evolution of the Paleo-Yangtze and Paleo-Red River

Recently, a number of review papers have attempted to reconstruct the evolution of Yangtze and Red River in the Cenozoic (Cao et al., 2023; Clift et al., 2020; Guo et al., 2021; Wissink et al., 2016; Z. Zhang, Daly, Li, et al., 2021; Z. Zhang, Daly, Yan, et al., 2021; P. Zhang et al., 2019; Z. Zhang et al., 2022; Zhao et al., 2021). These review papers all compiled databases either detrital zircon U–Pb ages, Sr–Nd isotopes, mica $^{40}\text{Ar}/^{39}\text{Ar}$ ages, or Pb isotopes of K-feldspar characterization. Yet, a consensus of opinion is yet to be reached. As noted in Section 1, most studies that suggest a through-flowing river from east Tibet to the South China Sea are based on the detection of similar detrital zircon U–Pb ages in different basins in southeast Tibet, all considered to be Greater paleo-Red River deposits. Our integrated provenance review of detrital zircon U–Pb data shows that the signatures of source areas of the east Qiangtang terrane, Songpan-Ganzi terrane, and Yidun Arc are indistinguishable after the Late Triassic due to zircon recycling and mixing. Therefore, the similar detrital zircon U–Pb spectra from many Cretaceous–Cenozoic basins in southeast Tibet as observed by many previous studies could be either the result of transportation by large rivers or recycling from local bedrock, and thus cannot be used as solid evidence to support the existence of a large through-flowing river in the Early Cenozoic. The integrated mica $^{40}\text{Ar}/^{39}\text{Ar}$ and Sr–Nd isotope data from the Cenozoic sediments and modern rivers in southeast Tibet have also not proved to be sensitive provenance discriminators thus far, mainly due to limited data or ambiguity of data

interpretations. Overall, the current provenance data determined from zircon U–Pb, mica $^{40}\text{Ar}/^{39}\text{Ar}$, and Sr–Nd are not sufficiently robust to support the Greater paleo-Red River capture model as many researchers suggested.

Detrital K-feldspar Pb isotopic signatures are currently the most promising avenue documented to determine if and when river capture occurred away from the Greater paleo-Red River. The clearest distinction between source signatures in the region lies in the recognition that the western Yangtze craton where the middle Yangtze flows has feldspars with a less radiogenic signature compared to the Red River (Clift et al., 2008; Z. Zhang et al., 2014). The presence of such grains in the paleo-Red River deposits would therefore indicate prior westward flow of the paleo-middle Yangtze into the Red River drainage, with the caveat that such grains can also be delivered to the Red River directly from Red River tributaries that drain the Yangtze craton, such as the Song Lo (Clift et al., 2008). The absence of these less radiogenic grains from the Eocene sediments in the onshore Hanoi Basin and the Eocene to Pliocene deposits of the offshore Yinggehai and Qiongdongnan basins suggests that the paleo-middle Yangtze had not flowed into the paleo-Red River at least since the late Eocene (Clift et al., 2008; Z. Zhang, Daly, Li, et al., 2021; Z. Zhang et al., 2017). The upper Yangtze k-feldspar signature, however, is less distinctive, with considerable overlap between signature fields of the Red River and upper Salween (Z. Zhang et al., 2017, 2023), making this method also insensitive to test whether the upper Yangtze was once connected to the Greater paleo-Red River in the Early Cenozoic.

Considering the different conclusions obtained using different/same provenance methods as shown in this study, it is unlikely to obtain an unambiguous conclusion regarding the drainage network evolution in the southeast margin of Tibet at this stage, but we would advocate that more $^{40}\text{Ar}/^{39}\text{Ar}$, Sr–Nd, and Pb isotope research on Cenozoic sediments in the southeast margin of Tibet, or a combination of these methods, could be effective in solving the Greater paleo-Red River capture model in the future.

6.2. Implications for Future Detrital Zircon U–Pb Provenance Studies in Southeast Tibet

We have shown in Sections 3 and 4 that sedimentary recycling plays a fundamental role in the source region detrital zircon signatures after the Late Triassic in southeast Tibet, which was not taken into account by most previous research that used detrital zircon U–Pb dating as a provenance tool to reconstruct paleo-drainage evolution in this region. We propose that after the amalgamation of various terranes (Qiangtang, Indochina, Sibumasu, Songpan–Ganzi) in the Middle–Late Triassic, the ongoing convergence resulted in significant orogeny within these terranes, allowing for the development of major rivers crossing the terranes and thus mixed provenance. The potential source terranes of the proposed upland Greater Paleo-Red River are therefore not easily differentiable in terms of having distinguishably different detrital zircon U–Pb spectra. Therefore, the use of detrital zircon U–Pb data in provenance studies to determine paleo-drainage evolution in this region remains challenging, and sedimentary recycling should be considered in more depth in future detrital zircon U–Pb studies in southeast Tibet.

Whilst this paper has focused largely on the role of sedimentary recycling in blurring the provenance signal, the potential degree of influence on the detrital zircon spectra of factors such as source region mineral fertility (e.g., Chew et al., 2020), the effect of hydraulic sorting and facies on the age spectrum (e.g., Malusà et al., 2016; Sun et al., 2020a; Yang et al., 2012), the number of grains required to adequately characterize a sample/site (e.g., Ibanez-mejia et al., 2018; Vermeesch, 2004) and analytical bias during experimental and data analysis (see review in Chew et al., 2020) could also be better considered in future studies for this region.

These aspects go beyond the scope of this paper to investigate in detail. However, we noted strong variations of detrital zircon U–Pb age spectra between different samples in the same formation in the Jianchuan Basin, and some samples only have very restricted age spectra (e.g., JSJ18 in Jinsichang Formation, Figure 10), which was previously interpreted as evidence of river capture (e.g., Yan et al., 2012). However, when multiple samples are analyzed from the same formation, the data suggest that intra-formational variability may simply record facies variation, with some samples continuing to reflect deposition from a through-flowing river (Figure 14). This interpretation is well illustrated by detrital zircon U–Pb data from the modern sediments at the First Bend of the Yangtze, which also show appreciable variation between different studies (Figures 13c–13g), which cannot be explained by river capture or provenance change. Moreover, initial apparent differences between the Shuanghe versus other Formations in the Jianchuan Basin, previously also interpreted as evidence of river capture (e.g., Feng et al., 2021), become less significant when the locally derived Cenozoic grains are excluded (Figures 11, 14f, and 15); this suggests that local input may create the illusion of provenance change while actually the regional input was still stable, and simply diluted.

7. Conclusions

In order to contribute to the long-disputed controversy on the drainage network reorganization in southeast Tibet and its link with Tibetan uplift, we compiled the detrital zircon U–Pb ages used as provenance signatures from the different terranes of southeastern Tibet, to which we added our own new data from the critical regions of the Gonjo and Jianchuan Basins. Our large compiled zircon U–Pb data set shows similar zircon U–Pb spectra between these terranes in upper Triassic and younger rocks, which makes it challenging to clearly distinguish between potential source signatures of the various terranes in southeast Tibet. This similarity of spectra makes it difficult to determine whether sedimentary rocks of the various Cenozoic basins in the region were locally derived or deposited by long-distance through-flowing rivers. Therefore, this presents a significant challenge in the use of detrital zircon U–Pb analyses as a provenance tool for documenting paleodrainage evolution in southeast Tibet.

Given the challenges of the zircon U–Pb approach in this setting, we sought to further explore the application of detrital mica $^{40}\text{Ar}/^{39}\text{Ar}$ analyses and Sr–Nd bulk analyses to this research question. We cautiously uphold the view that these techniques might have promise in certain regions. For example, the Sr–Nd signatures of the Jianchuan and Gonjo Basins are slightly different but with partial overlap, and in the region of the Jianchuan Basin, local rivers have a different Sr–Nd and mica $^{40}\text{Ar}/^{39}\text{Ar}$ signature to the modern upper Yangtze. However, there is some overlap between the Sr–Nd signatures of the modern Yangtze at the First Bend and the Red River at its source, and strong overlap in their mica $^{40}\text{Ar}/^{39}\text{Ar}$ signatures, which would also limit the use of these techniques in determining if the paleo-upper Yangtze ever flowed into the paleo-Red River. More analyses are needed to determine if this overlap is significant or is caused by outliers.

In total, our compiled large data set suggests that the current provenance data are not sufficiently conclusive to support the Greater paleo-Red River capture model as many researchers suggested when the influence of zircon sedimentary recycling, inter-sample variation, and local input are taken into consideration.

Data Availability Statement

All the data of this manuscript are accessible in the supporting information and will be made available on Zendo at Li et al. (2023) <https://zenodo.org/record/8152189> upon acceptance.

References

- Barbour, G. B. (1936). Physiographic history of the Yangtze. *The Geographical Journal*, 87(1), 17–32. <https://doi.org/10.2307/1786198>
- Brookfield, M. (1998). The evolution of the great river systems of southern Asia during the Cenozoic India-Asia collision: Rivers draining southwards. *Geomorphology*, 22(3–4), 285–312. [https://doi.org/10.1016/S0169-555X\(97\)00082-2](https://doi.org/10.1016/S0169-555X(97)00082-2)
- Bureau of Geology and Mineral Resources of Xizang (Tibet) Autonomous Region. (1993). Regional geology of Xizang (Tibet) autonomous region. In *Geological memoirs series*. Geological House.
- Cao, K., Leloup, P. H., Wang, G., Liu, W., Mahéo, G., Shen, T., et al. (2020). Thrusting, exhumation, and basin fill on the western margin of the South China block during the India-Asia collision. *Geological Society of America Bulletin*, 133(1–2), 74–90. <https://doi.org/10.1130/B35349.1>
- Cao, K., Leloup, P. H., Wang, G., Liu, W., Mahéo, G., Shen, T., et al. (2021). Thrusting, exhumation, and basin fill on the western margin of the South China block during the India-Asia collision. *GSA Bulletin*, 133(1–2), 74–90. <https://doi.org/10.1130/B35349.1>
- Cao, K., Wang, G., Leloup, P. H., Mahéo, G., Xu, Y., van der Beek, P. A., et al. (2019). Oligocene-Early Miocene topographic relief generation of southeastern Tibet triggered by thrusting. *Tectonics*, 38(1), 374–391. <https://doi.org/10.1029/2017tc004832>
- Cao, L., Shao, L., Qiao, P., Zhao, Z., & van Hinsbergen, D. J. J. (2018). Early Miocene birth of modern Pearl River recorded low-relief, high-elevation surface formation of SE Tibetan Plateau. *Earth and Planetary Science Letters*, 496, 120–131. <https://doi.org/10.1016/j.epsl.2018.05.039>
- Cao, L., Shao, L., van Hinsbergen, D. J., Jiang, T., Xu, D., & Cui, Y. (2023). Provenance and evolution of East Asian large rivers recorded in the East and South China Seas: A review. *Geological Society of America Bulletin* <https://doi.org/10.1130/B36559.1>
- Carter, A., Roques, D., Bristow, C., & Kinny, P. (2001). Understanding Mesozoic accretion in southeast Asia: Significance of Triassic tectonism (Indosinian orogeny) in Vietnam. *Geology*, 29(3), 211–214. [https://doi.org/10.1130/0091-7613\(2001\)029<0211:umaisa>2.0.co;2](https://doi.org/10.1130/0091-7613(2001)029<0211:umaisa>2.0.co;2)
- Chen, Y., Yan, M., Fang, X., Song, C., Zhang, W., Zan, J., et al. (2017). Detrital zircon U–Pb geochronological and sedimentological study of the Simao Basin, Yunnan: Implications for the Early Cenozoic evolution of the Red River. *Earth and Planetary Science Letters*, 476, 22–33. <https://doi.org/10.1016/j.epsl.2017.07.025>
- Chew, D., Sullivan, G., Caracciolo, L., Mark, C., & Tyrrell, S. (2020). Sourcing the sand: Accessory mineral fertility, analytical and other biases in detrital U–Pb provenance analysis. *Earth-Science Reviews*, 202, 103093. <https://doi.org/10.1016/j.earscirev.2020.103093>
- Chung, S.-L., Chu, M.-F., Zhang, Y., Xie, Y., Lo, C.-H., Lee, T.-Y., et al. (2005). Tibetan tectonic evolution inferred from spatial and temporal variations in post-collisional magmatism. *Earth-Science Reviews*, 68(3–4), 173–196. <https://doi.org/10.1016/j.earscirev.2004.05.001>
- Clark, M., House, M. A., Royden, L. H., Whipple, K. X., Burchfiel, B. C., Zhang, X., & Tang, W. (2005). Late Cenozoic uplift of southeastern Tibet. *Geology*, 33(6), 525–528. <https://doi.org/10.1130/g21265.1>
- Clark, M., Schoenbohm, L. M., Royden, L. H., Whipple, K. X., Burchfiel, B. C., Zhang, X., et al. (2004). Surface uplift, tectonics, and erosion of eastern Tibet from large-scale drainage patterns. *Tectonics*, 23(1), TC1006. <https://doi.org/10.1029/2002TC001402>

Acknowledgments

We are grateful to the Editor Harrison Gray, Prof. Ryan Leary and the other two anonymous reviewers for their helpful suggestions and comments, which have greatly improved our manuscript. The analysis of zircon U–Pb, mica $^{40}\text{Ar}/^{39}\text{Ar}$, and Sr–Nd isotopes was conducted when SL was a Royal Society postdoctoral researcher at Lancaster University. SL and YN acknowledge support from the Royal Society-K. C. Wong Fellowship and the NIGLFSC (award no. IP-1862-1118 to YN). This research is partly supported, for field work and sample preparation, by the National Natural Science Foundation of China (41888101 and 92155203). We thank Dr. Su Tao and Shen Zhongshan for field assistance and Dr Zhang Peng, Sun Xilin, and Licheng Cao for insightful discussions.

- Clift, P., Blusztajn, J., & Duc, N. A. (2006). Large-scale drainage capture and surface uplift in eastern Tibet-SW China before 24 Ma inferred from sediments of the Hanoi Basin, Vietnam. *Geophysical Research Letters*, 33(19), L19403. <https://doi.org/10.1029/2006GL027772>
- Clift, P., Layne, G., & Blusztajn, J. (2004). Marine sedimentary evidence for monsoon strengthening, Tibetan uplift and drainage evolution in East Asia. In P. D. Clift, W. Kuknt, P. X. Wang, & D. Hayes (Eds.), *Continent-ocean interactions within East Asian marginal seas* (Vol. 149, pp. 255–282). American Geophysical Union, Geophysical Monograph.
- Clift, P. D. (2016). Assessing effective provenance methods for fluvial sediment in the South China Sea. In P. D. Clift, J. Harff, J. Wu, & Q. Yan (Eds.), *River-dominated shelf sediments of East Asian Seas* (p. 429). Geological Society, London, Special Publications. <https://doi.org/10.1144/SP429.3>
- Clift, P. D., Carter, A., Campbell, I. H., Pringle, M. S., Van Lap, N., Allen, C. M., et al. (2006). Thermochronology of mineral grains in the Red and Mekong Rivers, Vietnam: Provenance and exhumation implications for southeast Asia. *Geochemistry, Geophysics, Geosystems*, 7(10), Q10005. <https://doi.org/10.1029/2006GC001336>
- Clift, P. D., Carter, A., Wysocka, A., Long, H. V., Zheng, H., & Neubeck, N. (2020). A Late Eocene–Oligocene through-flowing river between the Upper Yangtze and South China Sea. *Geochemistry, Geophysics, Geosystems*, 21(7), e2020GC009046. <https://doi.org/10.1029/2020gc009046>
- Clift, P. D., Long, H. V., Hinton, R., Ellam, R. M., Hannigan, R., Tan, M. T., et al. (2008). Evolving East Asian river systems reconstructed by trace element and Pb and Nd isotope variations in modern and ancient Red River-Song Hong sediments. *Geochemistry, Geophysics, Geosystems*, 9(4), Q04039. <https://doi.org/10.1029/2007GC001867>
- Cui, X., Jiang, X., Wu, H., & Xiong, G. (2011). Surface microscopic characteristics of quartz sand grains in the Paleogene Baoxiangsi Formation of Lijiang-Jianchuan area, northwestern Yunnan. *Geological Bulletin of China*, 30(8), 1238–1244.
- Deng, B., Chew, D., Jiang, L., Mark, C., Cogné, N., Wang, Z., & Liu, S. (2018). Heavy mineral analysis and detrital U–Pb ages of the intracontinental Paleo-Yangtze basin: Implications for a transcontinental source-to-sink system during Late Cretaceous time. *Geological Society of America Bulletin*, 130(11–12), 2087–2109. <https://doi.org/10.1130/b32037.1>
- Deng, B., Chew, D., Mark, C., Liu, S., Cogné, N., Jiang, L., et al. (2020). Late Cenozoic drainage reorganization of the paleo-Yangtze river constrained by multi-proxy provenance analysis of the Paleo-lake Xigeda. *Geological Society of America Bulletin*, 133(1–2), 199–211. <https://doi.org/10.1130/b35579.1>
- Ding, L., Yang, D., Cai, F., Pullen, A., Kapp, P., Gehrels, G., et al. (2013). Provenance analysis of the Mesozoic Hoh-Xil-Songpan-Ganzi turbidites in northern Tibet: Implications for the tectonic evolution of the eastern Paleo-Tethys Ocean. *Tectonics*, 32(1), 34–48. <https://doi.org/10.1002/tect.20013>
- Fan, D. D., Li, C. X., Yokoyama, K., Zhou, B. C., Li, B. H., Wang, Q., et al. (2005). Monazite age spectra in the Late Cenozoic strata of the Changjiang delta and its implication on the Changjiang run-through time. *Science in China—Series D: Earth Sciences*, 48(10), 1718–1727. <https://doi.org/10.1360/01yd0447>
- Faure, M., Nguyen, V. V., Hoai, L. T. T., & Lepvrier, C. (2018). Early Paleozoic or Early-Middle Triassic collision between the South China and Indochina blocks: The controversy resolved? Structural insights from the Kon Tum massif (Central Vietnam). *Journal of Asian Earth Sciences*, 166, 162–180. <https://doi.org/10.1016/j.jseaes.2018.07.015>
- Feng, Y., Song, C., He, P., Meng, Q., Wang, Q., Wang, X., & Chen, W. (2021). Detrital zircon U–Pb geochronology of the Jianchuan Basin, south-eastern Tibetan Plateau, and its implications for tectonic and paleodrainage evolution. *Terra Nova*, 33(6), 560–572. <https://doi.org/10.1111/ter.12548>
- Fox, M., Carter, A., & Dai, J. G. (2020). How continuous are the “relict” landscapes of southeastern Tibet? *Frontiers in Earth Science*, 8, 587597.
- Fu, X., Zhu, W., Geng, J., Yang, S., Zhong, K., Huang, X., et al. (2021). The present-day Yangtze River was established in the late Miocene: Evidence from detrital zircon ages. *Journal of Asian Earth Sciences*, 205, 104600. <https://doi.org/10.1016/j.jseaes.2020.104600>
- Gourbet, L., Leloup, P. H., Paquette, J.-L., Sorrel, P., Maheo, G., Wang, G., et al. (2017). Reappraisal of the Jianchuan Cenozoic basin stratigraphy and its implications on the SE Tibetan Plateau evolution. *Tectonophysics*, 700–701, 162–179. <https://doi.org/10.1016/j.tecto.2017.02.007>
- Guan, C., Yan, M. D., Zhang, W. L., Zhang, D. W., Fu, Q., Yu, L., et al. (2021). Paleomagnetic and chronologic data bearing on the Permian/Triassic boundary position of Qamdo in the eastern Qiangtang terrane: Implications for the closure of the Paleo-Tethys. *Geophysical Research Letters*, 48(6), e2020GL092059. <https://doi.org/10.1029/2020gl092059>
- Guo, R. J., Sun, X. L., Li, C. A., Li, Y. W., Wei, C. Y., Zhang, Z. J., et al. (2021). Cenozoic evolution of the Yangtze River: Constraints from detrital zircon U–Pb ages. *Palaeogeography, Palaeoclimatology, Palaeoecology*, 579, 110586. <https://doi.org/10.1016/j.palaeo.2021.110586>
- Hallet, B., & Molnar, P. (2001). Distorted drainage basins as markers of crustal strain east of the Himalaya. *Journal of Geophysical Research*, 106(B7), 13697–13709. <https://doi.org/10.1029/2000jb900335>
- He, M., Zheng, H., Bookhagen, B., & Clift, P. D. (2014). Controls on erosion intensity in the Yangtze River basin tracked by U–Pb detrital zircon dating. *Earth-Science Reviews*, 136, 121–140. <https://doi.org/10.1016/j.earscirev.2014.05.014>
- He, M., Zheng, H., & Clift, P. D. (2013). Zircon U–Pb geochronology and Hf isotope data from the Yangtze River sands: Implications for major magmatic events and crustal evolution in Central China. *Chemical Geology*, 360–361, 186–203. <https://doi.org/10.1016/j.chemgeo.2013.10.020>
- He, M., Zheng, H., Clift, P. D., Bian, Z., Yang, Q., Zhang, B., & Xia, L. (2021). Paleogene sedimentary records of the paleo-Jinshajiang (Upper Yangtze) in the Jianchuan Basin, Yunnan, SW China. *Geochemistry, Geophysics, Geosystems*, 22(6), e2020GC009500. <https://doi.org/10.1029/2020gc009500>
- Hoang, L., Clift, P. D., Mark, D., Zheng, H., & Tan, M. T. (2010). Ar–Ar muscovite dating as a constraint on sediment provenance and erosion processes in the Red and Yangtze River systems, SE Asia. *Earth and Planetary Science Letters*, 295(3–4), 379–389. <https://doi.org/10.1016/j.epsl.2010.04.012>
- Hoang, L., Wu, F.-Y., Clift, P. D., Wysocka, A., & Swierczewska, A. (2009). Evaluating the evolution of the Red River system based on in situ U–Pb dating and Hf isotope analysis of zircons. *Geochemistry, Geophysics, Geosystems*, 10(11), Q11008. <https://doi.org/10.1029/2009gc002819>
- Hoke, G. D., Liu-Zeng, J., Hren, M. T., Wissink, G. K., & Garzzone, C. N. (2014). Stable isotopes reveal high southeast Tibetan Plateau margin since the Paleogene. *Earth and Planetary Science Letters*, 394, 270–278. <https://doi.org/10.1016/j.epsl.2014.03.007>
- Horton, B. K., Yin, A., Spurlin, M. S., Zhou, J. Y., & Wang, J. H. (2002). Paleocene-Eocene syncontractional sedimentation in narrow, lacustrine-dominated basins of east-central Tibet. *Geological Society of America Bulletin*, 114(7), 771–786. [https://doi.org/10.1130/0016-7606\(2002\)114<0771:pessin>2.0.co;2](https://doi.org/10.1130/0016-7606(2002)114<0771:pessin>2.0.co;2)
- Huang, B., Yan, Y., Piper, J. D. A., Zhang, D., Yi, Z., Yu, S., & Zhou, T. (2018). Paleomagnetic constraints on the paleogeography of the East Asian blocks during Late Paleozoic and Early Mesozoic times. *Earth-Science Reviews*, 186, 8–36. <https://doi.org/10.1016/j.earscirev.2018.02.004>
- Ibañez-Mejía, M., Pullen, A., Pepper, M., Urbani, F., Ghoshal, G., & Ibañez-Mejía, J. C. (2018). Use and abuse of detrital zircon U–Pb geochronology—A case from the Río Orinoco delta, eastern Venezuela. *Geology*, 46, 1019–1022. <https://doi.org/10.1130/g45596.1>
- Jiao, R., Fox, M., & Yang, R. (2022). Late Cenozoic erosion pattern of the eastern margin of the Sichuan Basin: Implications for the drainage evolution of the Yangtze River. *Geomorphology*, 398, 108025. <https://doi.org/10.1016/j.geomorph.2021.108025>

- Kirby, E., Reiners, P. W., Krol, M. A., Whipple, K. X., Hodges, K. V., Farley, K. A., et al. (2002). Late Cenozoic evolution of the eastern margin of the Tibetan Plateau: Inferences from $^{40}\text{Ar}/^{39}\text{Ar}$ and (U-Th)/He thermochronology. *Tectonics*, *21*, 1–20. <https://doi.org/10.1029/2000tc001246>
- Kong, P., Granger, D., Wu, F., Caffee, M., Wang, Y., Zhao, X., & Zheng, Y. (2009). Cosmogenic nuclide burial ages and provenance of the Xigeda paleo-lake: Implications for evolution of the Middle Yangtze River. *Earth and Planetary Science Letters*, *278*(1–2), 131–141. <https://doi.org/10.1016/j.epsl.2008.12.003>
- Kong, P., Zheng, Y., & Caffee, M. W. (2012). Provenance and time constraints on the formation of the first bend of the Yangtze River. *Geochemistry, Geophysics, Geosystems*, *13*(6), Q06017. <https://doi.org/10.1029/2012gc004140>
- Lee, C. Y. (1934). The development of the upper Yangtze valley. *Bulletin of the Geological Society of China*, *13*(1), 107–118. <https://doi.org/10.1111/j.1755-6724.1934.mp13001006.x>
- Li, S., Deng, C. L., Yao, H. T., Huang, S., Liu, C. Y., He, H. Y., et al. (2013). Magnetostratigraphy of the Dali Basin in Yunnan and implications for late Neogene rotation of the southeast margin of the Tibetan Plateau. *Journal of Geophysical Research: Solid Earth*, *118*(3), 791–807. <https://doi.org/10.1002/jgrb.50129>
- Li, S., Hinsbergen, D. J. J., Shen, Z., Najman, Y., Deng, C., & Zhu, R. (2020). Anisotropy of magnetic susceptibility (AMS) analysis of the Gonjo Basin as an independent constraint to date Tibetan shortening pulses. *Geophysical Research Letters*, *47*(8), e2020GL087531. <https://doi.org/10.1029/2020gl087531>
- Li, S., Najman, Y., Vermeesch, P., Barfod, D. N., Millar, I., & Carter, A. (2023). A critical appraisal of the sensitivity of detrital zircon U–Pb provenance data to constrain drainage network evolution in southeast Tibet [Dataset]. Zenodo. <https://doi.org/10.5281/zenodo.8152189>
- Li, S., van Hinsbergen, D. J. J., Najman, Y., Liu-Zeng, J., Deng, C., & Zhu, R. (2020). Does pulsed Tibetan deformation correlate with Indian plate motion changes? *Earth and Planetary Science Letters*, *536*, 116144. <https://doi.org/10.1016/j.epsl.2020.116144>
- Li, S., Yin, C., Guilmette, C., Ding, L., & Zhang, J. (2019). Birth and demise of the Bangong–Nujiang Tethyan Ocean: A review from the Gerze area of central Tibet. *Earth-Science Reviews*, *198*, 102907. <https://doi.org/10.1016/j.earscirev.2019.102907>
- Li, S. H., Su, T., Spicer, R. A., Xu, C. L., Sherlock, S., Halton, A., et al. (2020). Oligocene deformation of the Chuandian terrane in the SE margin of the Tibetan Plateau related to the extrusion of Indochina. *Tectonics*, *39*(7), e2019TC005974. <https://doi.org/10.1029/2019tc005974>
- Liu, Z., Colin, C., Huang, W., Le, K. P., Tong, S., Chen, Z., & Trentesaux, A. (2007). Climatic and tectonic controls on weathering in South China and Indochina Peninsula: Clay mineralogical and geochemical investigations from the Pearl, Red, and Mekong drainage basins. *Geochemistry, Geophysics, Geosystems*, *8*(5), Q05005. <https://doi.org/10.1029/2006GC001490>
- Liu-Zeng, J., Zhang, J., McPhillips, D., Reiners, P., Wang, W., Pik, R., et al. (2018). Multiple episodes of fast exhumation since Cretaceous in southeast Tibet, revealed by low-temperature thermochronology. *Earth and Planetary Science Letters*, *490*, 62–76. <https://doi.org/10.1016/j.epsl.2018.03.011>
- Ma, Y., Yang, T., Bian, W., Jin, J., Wang, Q., Zhang, S., et al. (2018). A stable southern margin of Asia during the Cretaceous: Paleomagnetic constraints on the Lhasa–Qiangtang collision and the maximum width of the Neo-Tethys. *Tectonics*, *37*(10), 3853–3876. <https://doi.org/10.1029/2018tc005143>
- Malusà, M. G., Resentini, A., & Garzanti, E. (2016). Hydraulic sorting and mineral fertility bias in detrital geochronology. *Gondwana Research*, *31*, 1–19. <https://doi.org/10.1016/j.gr.2015.09.002>
- McPhillips, D., Hoke, G. D., Liu-Zeng, J., Bierman, P. R., Rood, D. H., & Niedermann, S. (2016). Dating the incision of the Yangtze River gorge at the First Bend using three-nuclide burial ages. *Geophysical Research Letters*, *43*(1), 101–110. <https://doi.org/10.1002/2015gl066780>
- Nie, J. S., Ruetenik, G., Gallagher, K., Hoke, G., Garzanti, C. N., Wang, W. T., et al. (2018). Rapid incision of the Mekong River in the middle Miocene linked to monsoonal precipitation. *Nature Geoscience*, *11*(12), 944–949. <https://doi.org/10.1038/s41561-018-0244-z>
- Nie, S. Y., Yin, A., Rowley, D. B., & Jin, Y. G. (1994). Exhumation of the Dabie-Shan ultra high-pressure rocks and accumulation of the Songpan-Ganzi flysch sequence, Central China. *Geology*, *22*(11), 999–1002. [https://doi.org/10.1130/0091-7613\(1994\)022<0999:eotdsu>2.3.co;2](https://doi.org/10.1130/0091-7613(1994)022<0999:eotdsu>2.3.co;2)
- Pullen, A., Kapp, P., Gehrels, G. E., Vervoort, J. D., & Ding, L. (2008). Triassic continental subduction in central Tibet and Mediterranean-style closure of the Paleo-Tethys Ocean. *Geology*, *36*(5), 351–354. <https://doi.org/10.1130/g24435a.1>
- Song, P., Ding, L., Li, Z., Lippert, P. C., Yang, T., Zhao, X., et al. (2015). Late Triassic paleolatitude of the Qiangtang block: Implications for the closure of the Paleo-Tethys Ocean. *Earth and Planetary Science Letters*, *424*, 69–83. <https://doi.org/10.1016/j.epsl.2015.05.020>
- Studnicki-Gizbert, C., Burchfiel, B. C., Li, Z., & Chen, Z. (2008). Early Tertiary Gonjo basin, eastern Tibet: Sedimentary and structural record of the early history of India-Asia collision. *Geos*, *4*, 713–735. <https://doi.org/10.1130/ges00136.1>
- Su, T., Spicer, R. A., Li, S.-H., Xu, H., Huang, J., Sherlock, S., et al. (2019). Uplift, climate and biotic changes at the Eocene–Oligocene transition in south-eastern Tibet. *National Science Review*, *0*(3), 1–10. <https://doi.org/10.1093/nsr/nwy062>
- Sun, X., Kuiper, K. F., Tian, Y., Li, C. A., Gemignani, L., Zhang, Z., & Wijbrans, J. R. (2020a). Impact of hydraulic sorting and weathering on mica provenance studies: An example from the Yangtze River. *Chemical Geology*, *532*, 119359. <https://doi.org/10.1016/j.chemgeo.2019.119359>
- Sun, X., Kuiper, K. F., Tian, Y., Li, C. A., Zhang, Z., Gemignani, L., et al. (2020b). $^{40}\text{Ar}/^{39}\text{Ar}$ mica dating of late Cenozoic sediments in SE Tibet: Implications for sediment recycling and drainage evolution. *Journal of the Geological Society*, *177*(4), 843–854. <https://doi.org/10.1144/jgs2019-099>
- Sun, X., Kuiper, K. F., Tian, Y., Li, C. A., Zhang, Z., & Wijbrans, J. R. (2020c). Comparison of Detrital zircon U–Pb and muscovite $^{40}\text{Ar}/^{39}\text{Ar}$ ages in the Yangtze sediment: Implications for provenance studies. *Minerals*, *10*(7), 643. <https://doi.org/10.3390/min10070643>
- Sun, X., Li, C. A., Kuiper, K. F., Wang, J., Tian, Y., Vermeesch, P., et al. (2017). Geochronology of detrital muscovite and zircon constrains the sediment provenance changes in the Yangtze River during the late Cenozoic. *Basin Research*, *30*(4), 636–649. <https://doi.org/10.1111/bre.12268>
- Sun, X., Tian, Y., Kuiper, K. F., Li, C. A., Zhang, Z., & Wijbrans, J. R. (2021). No Yangtze River prior to the Late Miocene: Evidence from detrital muscovite and K-feldspar $^{40}\text{Ar}/^{39}\text{Ar}$ geochronology. *Geophysical Research Letters*, *48*(5), e2020GL089903. <https://doi.org/10.1029/2020gl089903>
- Tang, M., Liu-Zeng, J., Hoke, G. D., Xu, Q., Wang, W., Li, Z., et al. (2017). Paleoelevation reconstruction of the Paleocene-Eocene Gonjo basin, SE-central Tibet. *Tectonophysics*, *712–713*, 170–181. <https://doi.org/10.1016/j.tecto.2017.05.018>
- Tian, Y., Kohn, B. P., Qiu, N., Yuan, Y., Hu, S., Gleadow, A. J. W., & Zhang, P. (2018). Eocene to Miocene out-of-sequence deformation in the eastern Tibetan Plateau: Insights from shortening structures in the Sichuan Basin. *Journal of Geophysical Research*, *123*(2), 1840–1855. <https://doi.org/10.1002/2017JB015049>
- Tian, Y., Liu, Y., Li, R., Sun, X., Zhang, Z., Carter, A., & Vermeesch, P. (2022). Thermochronological constraints on Eocene deformation regime in the Long-Men Shan: Implications for the eastward growth of the Tibetan Plateau. *Global and Planetary Change*, *217*, 103930. <https://doi.org/10.1016/j.gloplacha.2022.103930>
- Vermeesch, P. (2004). How many grains are needed for a provenance study? *Earth and Planetary Science Letters*, *224*(3–4), 441–451. <https://doi.org/10.1016/j.epsl.2004.05.037>
- Vermeesch, P. (2013). Multi-sample comparison of detrital age distributions. *Chemical Geology*, *341*, 140–146. <https://doi.org/10.1016/j.chemgeo.2013.01.010>

- Wallis, S., Tsujimori, T., Aoya, M., Kawakami, T., Terada, K., Suzuki, K., & Hyodo, H. (2003). Cenozoic and Mesozoic metamorphism in the Longmenshan orogen: Implications for geodynamic models of eastern Tibet. *Geology*, 31(9), 745–748. <https://doi.org/10.1130/g19562.1>
- Wang, E., Burchfiel, B. C., Royden, L. H., Chen, L. Z., Chen, J. S., Li, W. X., & Chen, Z. L. (1998). Late Cenozoic Xianshuihe-Xiaojiang, Red River, and Dali fault systems of southwestern Sichuan and Central Yunnan, China. *Geological Society of America Special Paper*, 327, 1–108.
- Wei, H.-H., Wang, E., Wu, G.-L., & Meng, K. (2016). No sedimentary records indicating southerly flow of the paleo-Upper Yangtze River from the First Bend in southeastern Tibet. *Gondwana Research*, 32, 93–104. <https://doi.org/10.1016/j.gr.2015.02.006>
- Wissink, G. K., Hoke, G. D., Garzzone, C. N., & Liu-Zeng, J. (2016). Temporal and spatial patterns of sediment routing across the southeast margin of the Tibetan Plateau: Insights from detrital zircon. *Tectonics*, 35(11), 2538–2563. <https://doi.org/10.1002/2016TC004252>
- Wu, F., Wan, B., Zhao, L., Xiao, W., & Zhu, R. (2020). Tethyan geodynamics. *Acta Petrologica Sinica*, 36(6), 1627–1674. <https://doi.org/10.18654/1000-0569/2020.06.01>
- Wu, Y., Fang, X., Liao, S., Xue, L., Chen, Z., Yang, J., et al. (2019). Zircon U-Pb geochronology of the Chinese continental crust: A preliminary analysis of the Elsevier science database. *Big Earth Data*, 3(1), 26–44. <https://doi.org/10.1080/20964471.2019.1576261>
- Xiao, R., Zheng, Y., Liu, X., Yang, Q., Liu, G., Xia, L., et al. (2021). Synchronous sedimentation in Gonjo Basin, Southeast Tibet in response to India-Asia collision constrained by magnetostratigraphy. *Geochemistry, Geophysics, Geosystems*, 22(3), e2020GC009411. <https://doi.org/10.1029/2020gc009411>
- Xiong, Z., Ding, L., Spicer, R. A., Farnsworth, A., Wang, X., Valdes, P. J., et al. (2020). The early Eocene rise of the Gonjo Basin, SE Tibet: From low desert to high forest. *Earth and Planetary Science Letters*, 543, 116312. <https://doi.org/10.1016/j.epsl.2020.116312>
- Yan, M., Zhang, D., Fang, X., Zhang, W., Song, C., Liu, C., et al. (2021). New insights on the age of the Mengyejing Formation in the Simao Basin, SE Tethyan domain and its geological implications. *Science China Earth Sciences*, 64(2), 231–252. <https://doi.org/10.1007/s11430-020-9689-3>
- Yan, Y., Carter, A., Huang, C.-Y., Chan, L.-S., Hu, X.-Q., & Lan, Q. (2012). Constraints on Cenozoic regional drainage evolution of SW China from the provenance of the Jianchuan Basin. *Geochemistry, Geophysics, Geosystems*, 13(3), Q03001. <https://doi.org/10.1029/2011gc003803>
- Yan, Z., Tian, Y., Li, R., Vermeesch, P., Sun, X., Li, Y., et al. (2019). Late Triassic tectonic inversion in the upper Yangtze Block: Insights from detrital zircon U-Pb geochronology from south-western Sichuan Basin. *Basin Research*, 31(1), 92–113. <https://doi.org/10.1111/bre.12310>
- Yang, R., Suhail, H. A., Gourbet, L., Willett, S. D., Fellin, M. G., Lin, X., et al. (2020). Early Pleistocene drainage pattern changes in Eastern Tibet: Constraints from provenance analysis, thermochronometry, and numerical modeling. *Earth and Planetary Science Letters*, 531, 115955. <https://doi.org/10.1016/j.epsl.2019.115955>
- Yang, R., Willett, S. D., & Goren, L. (2015). In situ low-relief landscape formation as a result of river network disruption. *Nature*, 520(7548), 526–529. <https://doi.org/10.1038/nature14354>
- Yang, S., Zhang, F., & Wang, Z. (2012). Grain size distribution and age population of detrital zircons from the Changjiang (Yangtze) River system, China. *Chemical Geology*, 296, 26–38. <https://doi.org/10.1016/j.chemgeo.2011.12.016>
- Yuan, X. P., Huppert, K. L., Braun, J., Shen, X., Liu-Zeng, J., Guertl, L., et al. (2021). Propagating uplift controls on high-elevation, low-relief landscape formation in the southeast Tibetan Plateau. *Geology*, 50(1), 60–65. <https://doi.org/10.1130/g49022.1>
- Yunnan Bureau of Geology and Mineral Resources (YBGMR). (1990). *Regional geology of Yunnan Province* (pp. 1–726). Geological Publishing House. (In Chinese).
- Zhang, H., Oskin, M. E., Liu-Zeng, J., Zhang, P., Reiners, P. W., & Xiao, P. (2016). Pulsed exhumation of interior eastern Tibet: Implications for relief generation mechanisms and the origin of high-elevation planation surfaces. *Earth and Planetary Science Letters*, 449, 176–185. <https://doi.org/10.1016/j.epsl.2016.05.048>
- Zhang, P., Najman, Y., Mei, L., Millar, I., Sobel, E., Carter, A., et al. (2019). Palaeodrainage evolution of the large rivers of East Asia, and Himalayan-Tibet tectonics. *Earth-Science Reviews*, 192, 601–630. <https://doi.org/10.1016/j.earscirev.2019.02.003>
- Zhang, Y., Huang, W., Huang, B., van Hinsbergen, D. J. J., Yang, T., Dupont-Nivet, G., & Guo, Z. (2018). 53–43 Ma deformation of the Eastern Tibet revealed by three stages of tectonic rotation in the Gongjue basin. *Journal of Geophysical Research: Solid Earth*, 123(5), 3320–3338. <https://doi.org/10.1002/2018jb015443>
- Zhang, Y., Huang, W., Zhang, Y., Poujol, M., Guillot, S., Roperch, P., & Guo, Z. (2019). Detrital zircon provenance comparison between the Paleocene-Eocene Nangqian-Xialaxiu and Gongjue basins: New insights for Cenozoic paleogeographic evolution of the eastern Tibetan Plateau. *Palaeogeography, Palaeoclimatology, Palaeoecology*, 533, 109241. <https://doi.org/10.1016/j.palaeo.2019.109241>
- Zhang, Z., Daly, J. S., Li, C. A., Tyrrell, S., Sun, X., Badenszki, E., et al. (2021). Formation of the Three Gorges (Yangtze River) no earlier than 10 Ma. *Earth-Science Reviews*, 216, 103601. <https://doi.org/10.1016/j.earscirev.2021.103601>
- Zhang, Z., Daly, J. S., Li, C. A., Tyrrell, S., Sun, X., & Yan, Y. (2017). Sedimentary provenance constraints on drainage evolution models for SE Tibet: Evidence from detrital K-feldspar. *Geophysical Research Letters*, 44(9), 4064–4073. <https://doi.org/10.1002/2017gl073185>
- Zhang, Z., Daly, J. S., Tian, Y., Tyrrell, S., Sun, X., Badenszki, E., et al. (2022). Sedimentary provenance perspectives on the evolution of the major rivers draining the eastern Tibetan Plateau. *Earth-Science Reviews*, 232, 104151. <https://doi.org/10.1016/j.earscirev.2022.104151>
- Zhang, Z., Daly, J. S., Tian, Y., Wang, Y., Badenszki, E., Sun, X., & Liu, Y. (2023). Sedimentary recycling in Jianchuan Basin, SE Tibetan Plateau: A solution to the debate on the formation age of the First Bend (Yangtze River). *Geomorphology*, 440, 108888. <https://doi.org/10.1016/j.geomorph.2023.108888>
- Zhang, Z., Daly, J. S., Yan, Y., Lei, C., Badenszki, E., Sun, X., & Tian, Y. (2021). No connection between the Yangtze and Red rivers since the late Eocene. *Marine and Petroleum Geology*, 129, 105115. <https://doi.org/10.1016/j.marpetgeo.2021.105115>
- Zhang, Z., Tyrrell, S., Li, C. A., Daly, J. S., Sun, X., & Li, Q. (2014). Pb isotope compositions of detrital K-feldspar grains in the upper-middle Yangtze River system: Implications for sediment provenance and drainage evolution. *Geochemistry, Geophysics, Geosystems*, 15(7), 2765–2779. <https://doi.org/10.1002/2014gc005391>
- Zhao, M., Shao, L., Liang, J., & Li, Q. (2015). No Red River capture since the late Oligocene: Geochemical evidence from the northwestern South China Sea. *Deep Sea Research Part II: Topical Studies in Oceanography*, 122, 185–194. <https://doi.org/10.1016/j.dsr2.2015.02.029>
- Zhao, X., Zhang, H., Hetzel, R., Kirby, E., Duvall, A. R., Whipple, K. X., et al. (2021). Existence of a continental-scale river system in eastern Tibet during the late Cretaceous-early Palaeogene. *Nature Communications*, 12(1), 7231. <https://doi.org/10.1038/s41467-021-27587-9>
- Zheng, H. (2015). Birth of the Yangtze River: Age and tectonic-geomorphic implications. *National Science Review*, 2(4), 438–453. <https://doi.org/10.1093/nsr/nwv063>
- Zheng, H., Clift, P. D., He, M., Bian, Z., Liu, G., Liu, X., et al. (2021). Formation of the First Bend in the late Eocene gave birth to the modern Yangtze River, China. *Geology*, 49(1), 35–39. <https://doi.org/10.1130/g48149.1>
- Zheng, H., Clift, P. D., Wang, P., Tada, R., Jia, J., He, M., & Jourdan, F. (2013). Pre-Miocene birth of the Yangtze River. *Proceedings of the National Academy of Sciences of the United States of America*, 110(19), 7556–7561. <https://doi.org/10.1073/pnas.1216241110>
- Zhou, D., & Graham, S. A. (1996). Songpan-Ganzi Triassic flysch complex of the West Qinling Shan as a remnant ocean basin. In A. Yin, & M. Harrison (Eds.), *The tectonic evolution of Asia* (pp. 281–299).